



LJMU Research Online

Ren, S, Liu, X, Gao, Y, Jing, R, Lin, P, Erkens, S and Wang, H

Molecular dynamics simulation and experimental validation on the interfacial diffusion behaviors of rejuvenators in aged bitumen

<http://researchonline.ljmu.ac.uk/id/eprint/19570/>

Article

Citation (please note it is advisable to refer to the publisher's version if you intend to cite from this work)

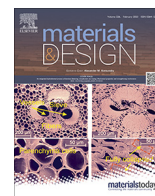
Ren, S, Liu, X, Gao, Y, Jing, R, Lin, P, Erkens, S and Wang, H (2023) Molecular dynamics simulation and experimental validation on the interfacial diffusion behaviors of rejuvenators in aged bitumen. *Materials and Design*. 226. ISSN 0264-1275

LJMU has developed **LJMU Research Online** for users to access the research output of the University more effectively. Copyright © and Moral Rights for the papers on this site are retained by the individual authors and/or other copyright owners. Users may download and/or print one copy of any article(s) in LJMU Research Online to facilitate their private study or for non-commercial research. You may not engage in further distribution of the material or use it for any profit-making activities or any commercial gain.

The version presented here may differ from the published version or from the version of the record. Please see the repository URL above for details on accessing the published version and note that access may require a subscription.

For more information please contact researchonline@ljmu.ac.uk

<http://researchonline.ljmu.ac.uk/>



Molecular dynamics simulation and experimental validation on the interfacial diffusion behaviors of rejuvenators in aged bitumen



Shisong Ren^a, Xueyan Liu^a, Yangming Gao^{a,*}, Ruxin Jing^a, Peng Lin^a, Sandra Erkens^a, Haopeng Wang^b

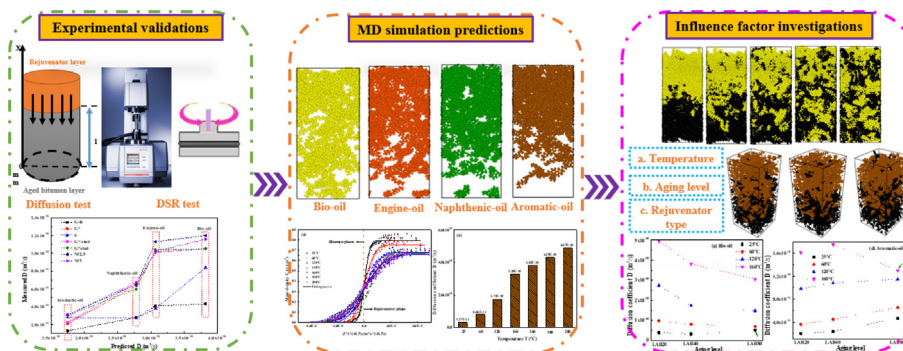
^a Section of Pavement Engineering, Faculty of Civil Engineering & Geosciences, Delft University of Technology, Stevinweg 1, 2628 CN Delft, the Netherlands

^b Nottingham Transportation Engineering Centre, University of Nottingham, Nottingham, UK

HIGHLIGHTS

- Molecular dynamics simulation was adopted to predict the interfacial diffusion coefficient of various rejuvenators in aged bitumen.
- The experimental results in both magnitude and order of diffusion coefficients agree well with MD simulation outputs.
- The magnitude for diffusion coefficients of four rejuvenators varies from 10^{-11} to 10^{-10} m²/s, and the diffusive capacity order is Bio-oil > Engine-oil > Naphthenic-oil > Aromatic-oil.
- The underlying mechanism comprises the free volume fraction distribution and intermolecular force between the rejuvenator and aged bitumen molecules.

GRAPHICAL ABSTRACT



ARTICLE INFO

Article history:

Received 5 September 2022

Revised 10 December 2022

Accepted 10 January 2023

Available online 11 January 2023

Keywords:

Diffusion behavior

Rejuvenator

Aged bitumen

Molecular dynamics simulation

Experimental validation

Influence factors

ABSTRACT

This study aims to multiscale investigate the effects of rejuvenator type, temperature, and aging degree of bitumen on the diffusion behaviors of rejuvenators (bio-oil BO, engine-oil EO, naphthenic-oil NO, and aromatic-oil AO) in aged binders. The molecular dynamics (MD) simulation method is performed to detect the molecular-level diffusion characteristics of rejuvenators and predict their diffusion coefficient (D) parameters. At an atomic scale, the mutual but partial interfacial diffusion feature between rejuvenators and aged bitumen molecules is observed. Moreover, Fick's Second Law well fits the concentration distribution of rejuvenator molecules in aged bitumen. The magnitude for D values of four rejuvenators varies from 10^{-11} to 10^{-10} m²/s, and the diffusive capacity order is BO > EO > NO > AO. Meanwhile, diffusion tests and dynamic shear rheometer (DSR) characterizations are employed to validate the MD simulation outputs. The experimental results in magnitude and order of D values agree well with MD simulation outputs. Lastly, the increased aging degree of bitumen exhibits a negative impact on the molecular diffusivity of BO, EO, and NO rejuvenators, while the D value of AO molecules enlarges as the aging level deepens. The underlying mechanism may be composed of the free volume fraction in aged bitumen and the intermolecular force between rejuvenator and aged bitumen molecules, which differs remarkably for various rejuvenators.

© 2023 The Authors. Published by Elsevier Ltd. This is an open access article under the CC BY license (<http://creativecommons.org/licenses/by/4.0/>).

* Corresponding author.

E-mail address: Y.Gao-3@tudelft.nl (Y. Gao).

1. Introduction

It is unavoidable for asphalt pavements to suffer from diverse distresses under heavy loading and environmental conditions [1,2]. Eventually, it is necessary to do the maintenance and reconstruction works on the damaged asphalt pavements. Afterward, a large amount of reclaimed asphalt pavement (RAP) is fabricated [3]. Considering both economic and environmental benefits, reusing these RAP materials in new asphalt pavements is attracting extensive attention [4,5]. Nevertheless, the amount of RAP materials in new asphalt mixture is limited and controlled because incorporating RAP without using soft bitumen or recycling agent would deteriorate the cracking and moisture damage resistance of asphalt pavements [6,7].

The main reasons for the high potential in both cohesive cracking and adhesive debonding of RAP material are attributed to the aged bitumen's considerable stiffness and moisture sensitivity [8]. Moreover, the aging mechanisms of bitumen are mainly composed of lightweight components' (saturates and aromatics) evaporation and conversion to heavy fractions (resins and asphaltenes) [9]. Meanwhile, the oxygen-containing functional groups (i.e., carbonyl and sulfoxide) are fabricated distinctly in bitumen molecules [10]. However, it is challenging to estimate these oxygen-containing functional groups due to the complexity of bitumen molecular components [11]. The supplement of lightweight oily components is the popular way to balance the concentration distribution of the saturates, aromatics, resins, and asphaltenes (SARA) fractions and to restore the rheological and mechanical performance of aged bitumen in RAP materials [12]. These oily additives are generally named rejuvenators or recycling agents.

However, it is hard to completely extract all bitumen binders from RAP materials and mix them with the rejuvenator in engineering practice [13]. The rejuvenators are always blended and integrated directly with the RAP mixtures [14]. In a rejuvenation procedure, the rejuvenator firstly attaches to the surface of aged bitumen on the RAP aggregates, then gradually diffuses into the aged bitumen layer until reaching a concentration equilibrium point and forming a homogenous rejuvenated bitumen [15]. Nevertheless, previous studies mentioned that partial blending between the rejuvenator and aged bitumen was observed in most RAP recycling cases [16,17]. At the same time, the blending level significantly affected the rejuvenation efficiency, and the heterogeneous distribution of rejuvenators in aged bitumen could result in a high occurrence potential of cracking and rutting distresses [18]. Therefore, it is crucial to guarantee a high blending between rejuvenators and aged bitumen quickly. In addition, it was reported that the blending degree was influenced by many material and environmental factors, such as the rejuvenator type, aging level of bitumen, and mixing temperature and time [19,20].

The blending degree of rejuvenated bitumen is strongly associated with the diffusive capacity of rejuvenators in aged bitumen, which is regularly evaluated by a diffusion coefficient parameter based on Fick's diffusion law [21]. Different experiments were conducted to measure the diffusion coefficient value of the rejuvenator in aged bitumen. Karlsson and Isacson [22] employed Fourier transform infrared spectroscopy by attenuated total reflectance (FTIR-ATR) method to detect the diffusion rate of the rejuvenator considering the influence of temperature, bitumen film thickness, bitumen type, and components. The findings demonstrated that the FTIR-ATR is an effective measurement for determining the diffusion coefficient values of rejuvenators in an aged bitumen matrix. The diffusion characteristics of rejuvenators observed agreed well with Fick's Law, and the Arrhenius formula was appropriate to describe the temperature effect on the

diffusion rate of rejuvenators in various aged binders when the temperature was above 30°C. Giacomo et al. [23] performed FTIR and dynamic shear rheometer (DSR) tests to monitor the diffusivity of rejuvenators in aged bitumen at 25°C and 140°C after a series of diffusion tests in tubes. The results revealed that the diffusion capacity strongly depended on the rejuvenator type and temperature. Fang et al. [24] also adopted a tube test to examine the D values of rejuvenators with variable temperatures and permeation times based on the viscosity variations during a diffusion process. It was reported that the increment in temperature and permeation time enlarged the permeation level of rejuvenators in aged bitumen. Moreover, the D values presented a decreasing trend with the increase in permeation time, which might be associated with reducing the permeation channel of rejuvenator molecules in aged bitumen. Ma et al. [25] performed a solvent extraction method to investigate the rejuvenator diffusion and distribution in various aged bitumen layers together with the penetration and DSR tests. The diffusive rate of rejuvenators in aged bitumen was remarkably attributed to the viscosity, components, and thermal stability. In addition, it was difficult for a rejuvenator to diffuse into the aged bitumen entirely within a short blending time.

Although these conventional characterization methods are able to qualitatively and quantitatively calculate the diffusion rates of rejuvenators in aged bitumen to a certain degree, they are time-consuming with an inevitable experimental error, and the underlying inner diffusion mechanisms at the nanoscale are still unclear. Nowadays, the molecular dynamics (MD) simulation method has been successfully employed in the diffusion measurement of rejuvenators in aged bitumen. Xu et al. [26] investigated the molecular diffusive behaviors of rejuvenators in neat, short-term, and long-term aged bitumen with an MD simulation. They concluded that both thermal molecular mobility and intermolecular force contributed to the relative diffusion rate of bitumen and rejuvenator molecules. In addition, the existence of micro-voids in the bitumen model and increased temperature also benefited the fusion level of rejuvenator molecules. Meanwhile, Xu and Wang [27] also performed an MD simulation to explore the diffusion and interaction mechanisms of rejuvenator molecules in virgin and aged bitumen. The rejuvenator improved the blending level between virgin and aged bitumen, which diffused more into pure bitumen than the aged binder, contrary to a previous conclusion [26]. Based on MD simulation outputs, Sun and Wang [28] found that the diffusion capacity of rejuvenator molecules in the aged bitumen model distinctly relied on the rejuvenator's molecular structure. The polar aromatic exhibited the worst diffusive capacity, while naphthene aromatic showed a faster diffusion rate than saturate-based rejuvenators. The positive effect of bio-rejuvenators on accelerating the fusion process between virgin and aged bitumen was also reported in an MD simulation research [29].

In view of the literature review, there are still many research gaps regarding the diffusion and blending characteristics of rejuvenators in the aged bitumen layer of RAP materials. Some of them are listed as follows:

- Although it has been proved that the MD simulation method is an efficient way to predict the diffusion coefficient of a rejuvenator in an aged bitumen system, the commonly-used molecular models of various rejuvenators are generally based on previous literature rather than their realistic components measured from chemical tests.
- There is few MD simulation study on the diffusion behaviors of rejuvenators in aged bitumen, and the corresponding underlying mechanism at an atomic scale is still unclear.

- Currently, most MD simulations and experimental investigations on the diffusion capacity of rejuvenators in aged bitumen are separated, and the connection between MD simulation outputs and experimental results has not been built yet.
- The coupled influence of rejuvenator components, temperature, and aging degree of bitumen on the diffusion capacity of rejuvenators in aged bitumen has not been investigated systematically.

2. Research objective and structure

This study predicts and compares the diffusion behaviors of commonly-used rejuvenators in aged binders at variable aging levels at different temperatures. Fig. 1 illustrates the primary research protocol. First, the molecular models of aged bitumen and four different rejuvenators (bio-oil, engine-oil, naphthenic-oil, and aromatic-oil) are built based on their chemical characteristics. Afterwards, four rejuvenator-aged bitumen bi-layer diffusion molecular models are established for MD simulations at different temperatures of 25, 60, 120, 140, 160, 180, and 200 °C. The molecular-scale diffusion phenomena of various rejuvenators in aged bitumen are observed and compared. Finally, analysing the mass density profile of rejuvenators in aged bitumen layers, the diffusion coefficient (D) values of four rejuvenators at different temperatures are predicted. In addition, the activation energy (Ea) and pre-exponential factor (A) parameters are derived based on these predicted D parameters.

On the other hand, the diffusion tube tests with these four rejuvenators in aged bitumen are conducted at 160 °C. The concentration distributions of rejuvenators are determined using the standard curves between the rheological parameters and rejuvenator concentration from the dynamic shear rheometer (DSR) tests. The experimental results of D, Ea, and A are compared with MD simulation outputs to estimate the application potential of the MD simulation method in predicting the diffusive capacity of various rejuvenators in an aged binder. Finally, the influence of rejuvenator type, diffusion temperature, and aging degree of bitumen on the diffusion behaviors of rejuvenators in aged binders are investigated.

3. Materials and methods

3.1. Bitumen and rejuvenators

This study utilized a Total 70/100 virgin bitumen in aging, rejuvenation, and diffusion tests. Table 1 lists the basic properties of virgin bitumen. Meanwhile, four types of commonly-used rejuvenators were selected, including the bio-oil (BO), engine-oil (EO), naphthenic-oil (NO), and aromatic-oil (AO). Their chemical and physical properties are summarized in Table 2. It should be mentioned that the selection basis of rejuvenators is the classification list from the American National Centre of Asphalt Technology (NCAT) [30], in which the rejuvenators are divided into five groups: paraffinic oils, aromatic extracts, naphthenic oils, triglycerides & fatty acids, and tall oils [31]. In addition, the bio-oil rejuvenator selected in this study is rapeseed oil derived from a transesterification process.

Table 2 shows the chemical and physical properties of four rejuvenators. It can be observed that the aromatic-oil exhibits the highest density, viscosity, C/H ratio, and average molecular weight values, while the engine-oil shows the lowest values in density. The order in both viscosity and molecular weight for four rejuvenators is the same as BO < EO < NO < AO. Moreover, the bio-oil rejuvenator presents a specific characteristic of a large oxygen amount associated with the ester group in its molecular structure [39]. In addition, an extremely slight amount of sulfur and nitrogen elements are observed in all four rejuvenators.

3.2. Laboratory aging procedure of bitumen

The virgin bitumen was subjected both to short-term and long-term aging to obtain the aged bitumen. Firstly, about 50 g of virgin bitumen in an aluminium plate was put in an oven at 163°C for 5 h to simulate the short-term aging during the mixing and compaction processes [40]. Afterwards, the short-term aged bitumen was moved into the Pressure Aging Vessel (PAV) to further long-term aging for 20, 40, and 80 h with the pressure and temperature of 2.1 MPa and 100°C, respectively [41]. To simplify, the aged bitu-

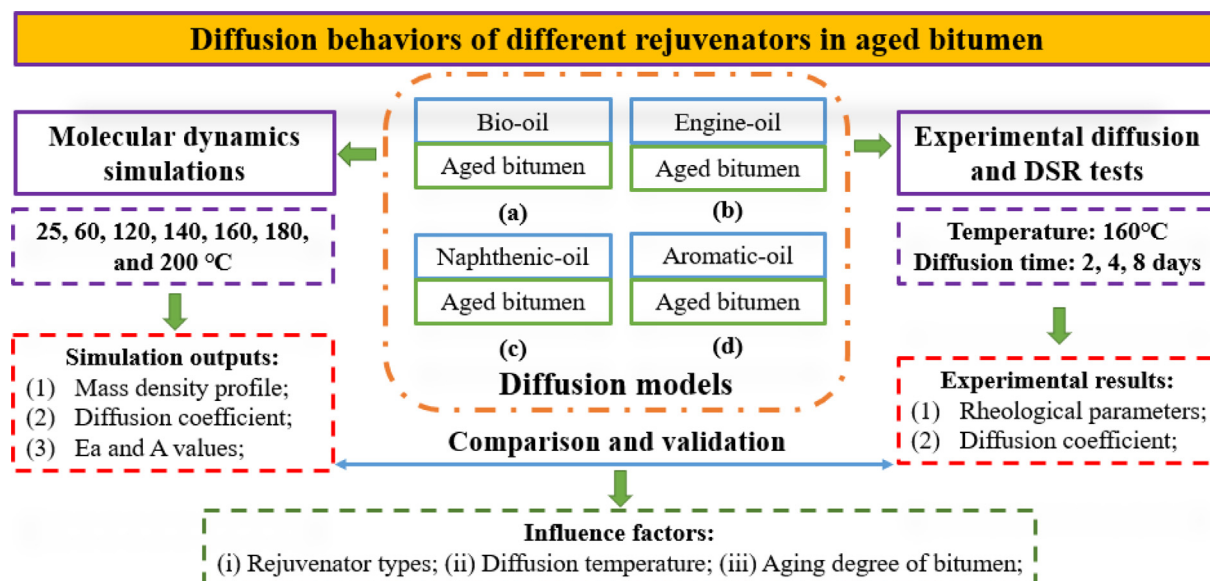


Fig. 1. Research scheme and structure.

Table 1
Basic properties of Total 70/100 virgin bitumen.

| Properties | value | Test standard | |
|--|--------------------|------------------|-----------------|
| 25°C Penetration (1/10 mm) | 91 | ASTM D5 [32] | |
| Softening point (°C) | 48 | ASTM D36 [33] | |
| 135°C Dynamic viscosity (Pa•s) | 0.8 | AASHTO T316 [34] | |
| 25°C Density (g/cm ³) | 1.017 | EN 15,326 [35] | |
| 60°C Density (g/cm ³) | 0.996 | | |
| Chemical fractions (wt%) | Saturate, S | 3.6 | |
| | Aromatic, A | 53.3 | |
| | Resin, R | 30.3 | |
| | Asphaltene, As | 12.8 | |
| | Colloidal index CI | 0.196 | |
| Element compositions (wt%) | Carbon, C | 84.06 | ASTM D7343 [37] |
| | Hydrogen, H | 10.91 | |
| | Oxygen, O | 0.62 | |
| | Sulfur, S | 3.52 | |
| | Nitrogen, N | 0.9 | |
| Complex shear modulus at 1.6 Hz & 60°C (kPa) | 2.4 | AASHTO M320 [38] | |
| Phase angle at 1.6 Hz & 60°C (°) | 84.5 | | |

men with long-term aging times of 20, 40, and 80 h are abbreviated as LAB20, LAB40, and LAB80.

3.3. Preparation of rejuvenated bitumen

In this study, the calibration curves between the rheological indices and rejuvenator dosage should be first drawn to determine the concentration distribution of rejuvenators in different aged bitumen layers and calculate the corresponding diffusion coefficient value [23,24,42]. To this end, rejuvenated bitumen binders were prepared with variable rejuvenator types and dosages. The LAB40-aged bitumen was heated to a flow state and blended with a rejuvenator for 15 min to prepare the homogenous rejuvenated binders. The rejuvenator dosages were 2.5, 5.0, 7.5, 10.0, 12.5, and 15.0 wt%. The prepared rejuvenated binders were preserved at low temperatures for rheology tests. Further, the bio-oil, engine-oil, naphthenic-oil, and aromatic-oil rejuvenated bitumen are marked as the BORB, EORB, NORB, and AORB, respectively.

3.4. Characterization methods

3.4.1. Experimental diffusion tests

In this study, the experimental results in diffusion coefficient values of four rejuvenators in aged bitumen were measured to verify the MD simulation outputs. Based on previous studies [23,24], the tube test was adopted to conduct the diffusion measurements of rejuvenator-aged bitumen bi-layers, as shown in Fig. 2. About

Table 2
Chemical and physical properties of four rejuvenators.

| Rejuvenators | Bio-oil | Engine-oil | Naphthenic-oil | Aromatic-oil |
|-------------------------------------|--------------------|--------------|--------------------|-----------------------|
| Appearance | Pale-yellow liquid | Brown liquid | Transparent-liquid | Dark-brown half-solid |
| 25°C Density (g/cm ³) | 0.911 | 0.833 | 0.875 | 0.994 |
| 60°C Density (g/cm ³) | 0.899 | 0.814 | 0.852 | 0.978 |
| 25°C viscosity (cP) | 50 | 60 | 130 | 63,100 |
| Flash point (°C) | > 250 | > 225 | > 230 | > 210 |
| Carbon C (wt%) | 76.47 | 85.16 | 86.24 | 88.01 |
| Hydrogen H (wt%) | 11.96 | 14.36 | 13.62 | 10.56 |
| Oxygen O (wt%) | 11.36 | 0.12 | 0.10 | 0.40 |
| Sulfur S (wt%) | 0.06 | 0.13 | 0.10 | 0.48 |
| Nitrogen N (wt%) | 0.15 | 0.23 | 0.12 | 0.55 |
| Average molecular weight Mn (g/mol) | 286.43 | 316.48 | 357.06 | 409.99 |

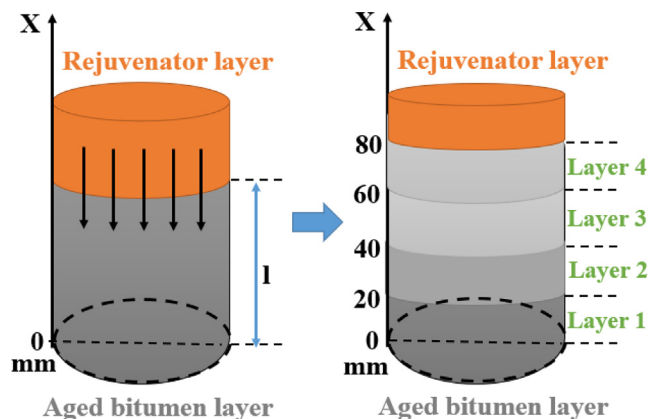


Fig. 2. The schematic graph of the diffusion process of rejuvenator in aged bitumen.

40 g of aged bitumen was poured into a cylindrical aluminium foil tube with a diameter of 13 mm and a height of 100 mm. When the aged bitumen sample was cooled to room temperature, a 4 g rejuvenator (10 wt% of aged bitumen) was incorporated into the upper layer. Afterwards, the nozzle was sealed with foil paper to avoid the evaporation and oxidation of the rejuvenator during a thermal diffusion procedure. Twelve diffused samples were prepared and vertically placed in an oven at 160°C. All specimens were divided into three groups in line with the variable diffusion times of 2, 4, and 8 days.

Once the diffusion process ended, the sample was removed from the oven to a refrigerator at -20°C to discontinue the diffusion process and solidify these diffused specimens for further isometric cutting. After removing it from the fridge, the aluminium foil tube was ripped off manually. As illustrated in Fig. 2, the diffused sample was marked and cut into four layers with a height of 20 mm by a hot knife. It should be mentioned that the tube bottom was set as the origin point. It was challenging to distinguish the rejuvenator phase from bitumen at an interface zone because the interfacial diffusion was bidirectional. On the contrary, the bottom aged bitumen layer with a bit of rejuvenator was still hard at room temperature. Each layer on an aluminium plate was ultimately heated and homogenized carefully for rejuvenator concentration determination using rheological characterizations.

In line with the previous study [23], an immediate solution of Fick's second Law is employed to describe the relationship between the rejuvenator concentration with diffusion time and distance, as shown in Eq.1. It is assumed that the surface concen-

tration C_1 is constant with time, and the initial concentration C_0 in the sample equals zero.

$$\frac{C(t) - C_0}{C_1 - C_0} = 1 - \frac{4}{\pi} \times \sum_{n=0}^{\infty} \left[\frac{(-1)^n}{2n+1} \exp\left\{ \frac{-D(2n+1)^2 \pi^2 t}{4l^2} \right\} \cos\left\{ \frac{(2n+1)\pi x}{2l} \right\} \right] \quad (1)$$

where $C(t)$ refers to the rejuvenator concentration at diffusion time t , wt%; C_0 and C_1 are the initial and final concentrations of the rejuvenator, which are assumed to be 100 wt% and 0; D represents the diffusion coefficient, m^2/s ; t (s) and l (m) shows the diffusion time and the tube length filled with bitumen; the x denotes the abscissa where the rejuvenator concentration $C(t)$ is calculated.

When an assumption is adopted that the C_0 is equal to zero, **Eq.1** can be simplified as follows:

$$C(t) = C_1 - \frac{4}{\pi} C_1 \times \sum_{n=0}^{\infty} \left[\frac{(-1)^n}{2n+1} \exp\left\{ \frac{-D(2n+1)^2 \pi^2 t}{4l^2} \right\} \cos\left\{ \frac{(2n+1)\pi x}{2l} \right\} \right] \quad (2)$$

From **Eq.2**, it is found that the rejuvenator concentration $C(t)$ varies as a function of diffusion time (t) and position (x). Thus, the diffusion coefficient D values can be derived by fitting these correlation curves.

3.4.2. Dynamic shear rheometer (DSR) test

The rheological properties of each diffusion layer were measured through a DSR device with a plate diameter of 8 mm and

thickness of 2 mm [38]. All rejuvenated bitumen and diffused samples were subjected to a frequency sweep test, Glover-Rowe (G-R) parameter measurement, and linear amplitude sweep (LAS) test. The frequency sweep tests were conducted at 20°C with the frequency rising from 0.1 rad/s to 100 rad/s. Moreover, the G-R parameter was measured at 15 °C and 0.005 rad/s. Besides, all LAS tests were carried out at 20°C to obtain the life cycles at 2.5 % and 5.0 % strain levels according to AASHTO TP 101 [43]. It should be noted that each rheological test for all samples was performed at least two times to guarantee the reliability of experimental data.

4. Molecular dynamics simulations

4.1. Molecular model of aged bitumen

The most popular 12-component molecular model is adopted as the virgin bitumen model. During a thermo-oxidative aging process, polar oxygen-containing functional groups are introduced in bitumen molecules, such as carbonyl and sulfoxide. Hence, the oxidized molecular structures of aromatic, resin, and asphaltene molecules are built, while the chemical structure of saturate molecules has no change. The detailed principle for determining the molecular structures in aged bitumen can be found in our previous study [44]. **Fig. 3** illustrates the molecular structures of chemical components in virgin and aged bitumen models. It should be mentioned that the molecular appellations are superscripted as “0–4” to distinguish the SARA molecules with variable oxidative aging degrees.

Before establishing the molecular models of aged bitumen, the number of each molecule is resolved according to the experimental results in both molecular weight ratio and SARA fractions distribution, which are listed in **Table 3**. More related information can be

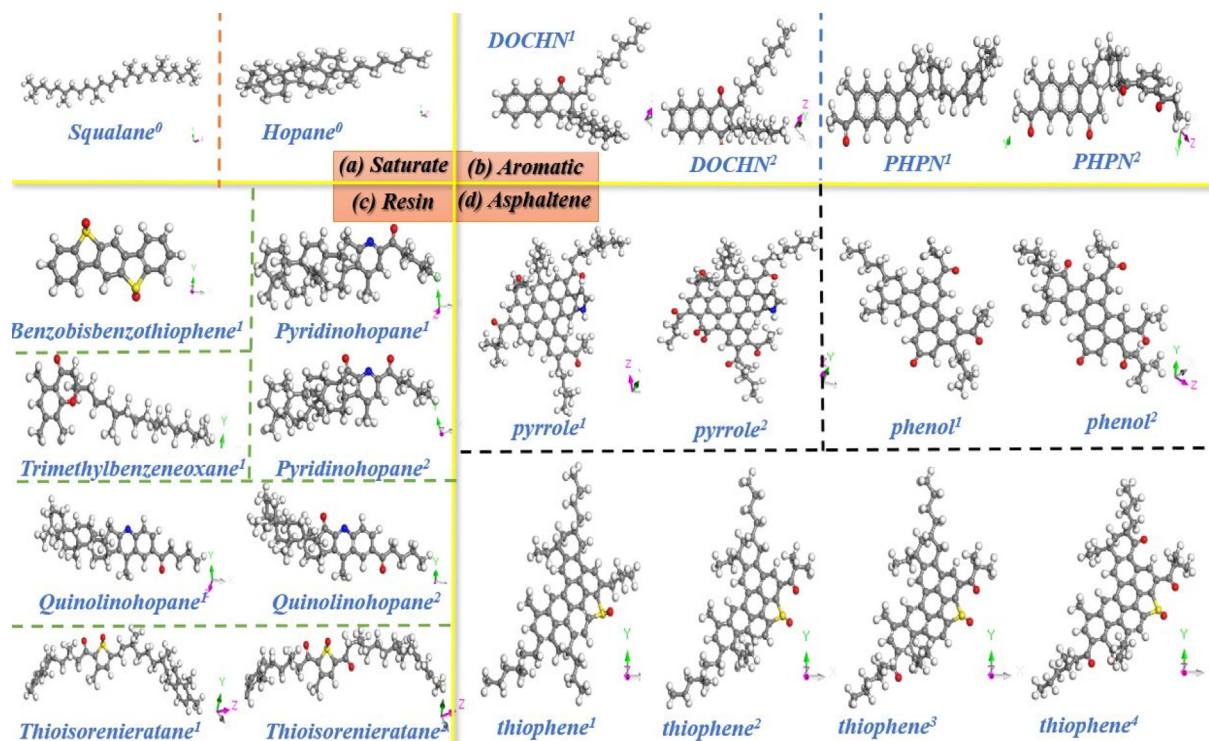


Fig. 3. Chemical components in the molecular model of various aged binders.

Table 3
The number of SARA molecules in molecular models of various aged bitumen.

| Chemical fractions | Molecular structure | Chemical formula | LAB20 | LAB40 | LAB80 |
|-------------------------------------|-----------------------------------|---|-----------------------------------|-------|-------|
| Saturate | Squalane ⁰ | C ₃₀ H ₆₂ | 2 | 2 | 2 |
| | Hopane ⁰ | C ₃₅ H ₆₂ | 1 | 1 | 1 |
| Aromatic | PHPN ⁰ | C ₃₅ H ₄₄ | 12 | 0 | 0 |
| | PHPN ¹ | C ₃₅ H ₄₂ O | 6 | 15 | 0 |
| | PHPN ² | C ₃₅ H ₃₆ O ₄ | 0 | 0 | 13 |
| | DOCHN ⁰ | C ₃₀ H ₄₆ | 17 | 0 | 0 |
| | DOCHN ¹ | C ₃₀ H ₄₄ O | 0 | 16 | 0 |
| | DOCHN ² | C ₃₀ H ₄₂ O ₂ | 0 | 0 | 13 |
| | Resin | Quinolinhopane ⁰ | C ₄₀ H ₅₉ N | 4 | 0 |
| Quinolinhopane ¹ | | C ₄₀ H ₅₇ NO | 0 | 5 | 0 |
| Quinolinhopane ² | | C ₄₀ H ₅₅ NO ₂ | 0 | 0 | 5 |
| Thioisorenieratane ¹ | | C ₄₀ H ₅₈ SO ₂ | 3 | 3 | 0 |
| Thioisorenieratane ² | | C ₄₀ H ₅₆ SO ₃ | 0 | 0 | 3 |
| Benzobisbenzothiophene ¹ | | C ₁₈ H ₁₀ S ₂ O ₂ | 13 | 14 | 15 |
| Pyridinohopane ⁰ | | C ₃₆ H ₅₇ N | 4 | 0 | 0 |
| Pyridinohopane ¹ | | C ₃₆ H ₅₅ NO | 0 | 4 | 0 |
| Pyridinohopane ² | | C ₃₆ H ₅₃ NO ₂ | 0 | 0 | 5 |
| Trimethylbenzeneoxane ⁰ | | C ₂₉ H ₅₀ O | 4 | 5 | 0 |
| Trimethylbenzeneoxane ¹ | | C ₂₉ H ₄₈ O ₂ | 0 | 0 | 6 |
| Asphaltene-phenol ⁰ | | C ₄₂ H ₅₄ O | 3 | 0 | 0 |
| Asphaltene-phenol ¹ | | C ₄₂ H ₄₈ O ₄ | 0 | 4 | 0 |
| Asphaltene-phenol ² | | C ₄₂ H ₄₄ O ₆ | 0 | 0 | 4 |
| Asphaltene-pyrrole ⁰ | | C ₆₆ H ₈₁ N | 3 | 0 | 0 |
| Asphaltene-pyrrole ¹ | | C ₆₆ H ₇₃ NO ₄ | 0 | 3 | 0 |
| Asphaltene-pyrrole ² | | C ₆₆ H ₆₇ NO ₇ | 0 | 0 | 4 |
| Asphaltenes | Asphaltene-thiophene ² | C ₅₁ H ₆₀ SO ₂ | 3 | 0 | 0 |
| | Asphaltene-thiophene ³ | C ₅₁ H ₅₈ SO ₃ | 0 | 3 | 0 |
| | Asphaltene-thiophene ⁴ | C ₅₁ H ₅₄ SO ₅ | 0 | 0 | 4 |

found in our previous paper [44]. It is demonstrated that the mass percentages of saturate, aromatic, resin, and asphaltene molecules in all molecular models of aged bitumen match well with measured values, which guarantees the reliability of molecular models and MD simulation outputs.

4.2. Molecular models of different rejuvenators

In this study, the average molecular structures of four rejuvenators are determined based on their chemical characteristics of elemental analysis, functional group distribution, and average molecular weight. Our previous paper described how to construct the average molecular structures of these rejuvenators [45], as illustrated in Fig. 4. The chemical formulas of BO, EO, NO, and AO rejuvenators are C₁₉H₃₆O₂, C₂₂H₄₄, C₂₆H₄₈, and C₃₀H₄₀. It demonstrates that the molecular structure of BO is composed of one straight monoalkene chain and an ester group. Moreover, the EO rejuvenator shows one cyclohexane structure with two saturated

n-octane side chains. The main body in NO is the saturated tricyclic alkanes linked with *n*-hexane and *n*-heptane alkyl substituents. In addition, the AO rejuvenator presents a molecular centre of polycyclic aromatic hydrocarbon structure connected with a saturated straight-chain and monocyclic alkanes. It was revealed that these four rejuvenators from various categories exhibited diverse chemical, physical, and thermodynamic properties, which contributed to a significant difference in their diffusion behaviors in aged bitumen [28].

0.4.3. Bulk and confined molecular models of aged bitumen and rejuvenators.
The bulk molecular models of aged bitumen and four rejuvenators with a density of 0.1 g/cm³ are built first. It should be mentioned that in each rejuvenator model, the number of rejuvenator molecules is the same as 200. The geometry optimizations are carried out on these molecular models to eliminate the intermolecular overlaps and seek stable configurations with minimum energy. Afterwards, these initial configurations are subjected to the MD simulations with an isothermal-isobaric ensemble (constant atom

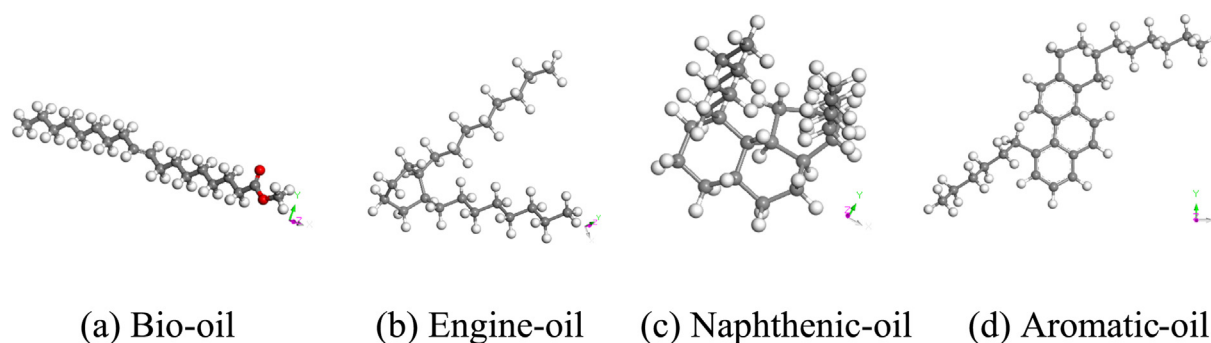


Fig. 4. Average molecular structures of four rejuvenators (Carbon atoms: black; Hydrogen atoms: white; Oxygen atoms: red). (For interpretation of the references to colour in this figure legend, the reader is referred to the web version of this article.)

number N , pressure P , and temperature T) for 200 picoseconds (ps) at 298 K and one-atmosphere pressure. The time step is set as 1 fs (fs), while the Nose thermostat and Andersen barostat are adopted to control the temperature and pressure. At the same time, the summation methods for the van der Waals and the electrostatic terms are Atom-based with a cut-off distance of 15.5 Å and Ewald with an accuracy of 0.001 kcal/mol. To further equilibrate the molecular models of aged bitumen and rejuvenators, the additional MD simulations with a canonical ensemble (constant molecular number N , cell volume V , and temperature T) at 298 K for 200 ps. Furthermore, the confined molecular models of aged bitumen and rejuvenators are established and equilibrated like the MD simulations on bulk systems. The only difference between the confined and bulk model is the boundary condition, and the periodic boundary condition is adopted in bulk models. For confined models, the periodic boundary condition is applied in both the x and y directions, while the non-periodic boundary condition is selected in the z -direction.

Fig. 5 shows the confined molecular models of aged bitumen and rejuvenator after NPT and NVT equilibrium MD simulations. In the meantime, the bi-layer rejuvenator-aged bitumen diffusion model is established through a layer-construction tool. A vacuum layer of 5 Å is added on the top of the diffusion model to block up the molecular interaction between adjacent simulation cells at the z -direction, as illustrated in Fig. 5 with a dimension of 40 Å × 40 Å × 107 Å. It should be noted that all MD simulations on bulk, confined, and bi-layer molecular models are performed with a Polymer Consistent Force Field (PCFF), which has been

widely employed and validated in polymers, organic, and bituminous materials [46].

4.3. MD simulations on rejuvenator-aged bitumen diffusion models

All rejuvenator-aged bitumen diffusion models in this study are built using Materials Studio. Fig. 6 displays the BO-aged bitumen, EO-aged bitumen, NO-aged bitumen, and AO-aged bitumen interfacial models. The MD simulations on all diffusion models are completed in a Large-scale Atomic/Molecular Massively Parallel Simulator (LAMMPS) with an NVT ensemble and Nose-Hoover thermostat. Meanwhile, the time step and simulation duration are 1 fs and 10 ns, which are sufficient to observe the diffusion behavior and calculate the diffusion coefficient values of rejuvenators in aged bitumen. The atomic trajectories of the rejuvenator molecules in diffusion models are viewed through a visualization tool OVITO. During the diffusion simulations, the density distribution of rejuvenator molecules in a whole diffusion model is monitored instantly to derive the diffusion coefficient parameter.

4.4. Validations on MD simulation outputs

Apart from the diffusion models, MD simulations are also carried out on various bulk models of virgin bitumen, aged bitumen, and rejuvenators to verify the reliability of molecular models and simulation set parameters. This section compares the predicted density values of all bitumen and rejuvenator models with experimental results, as listed in Table 4.

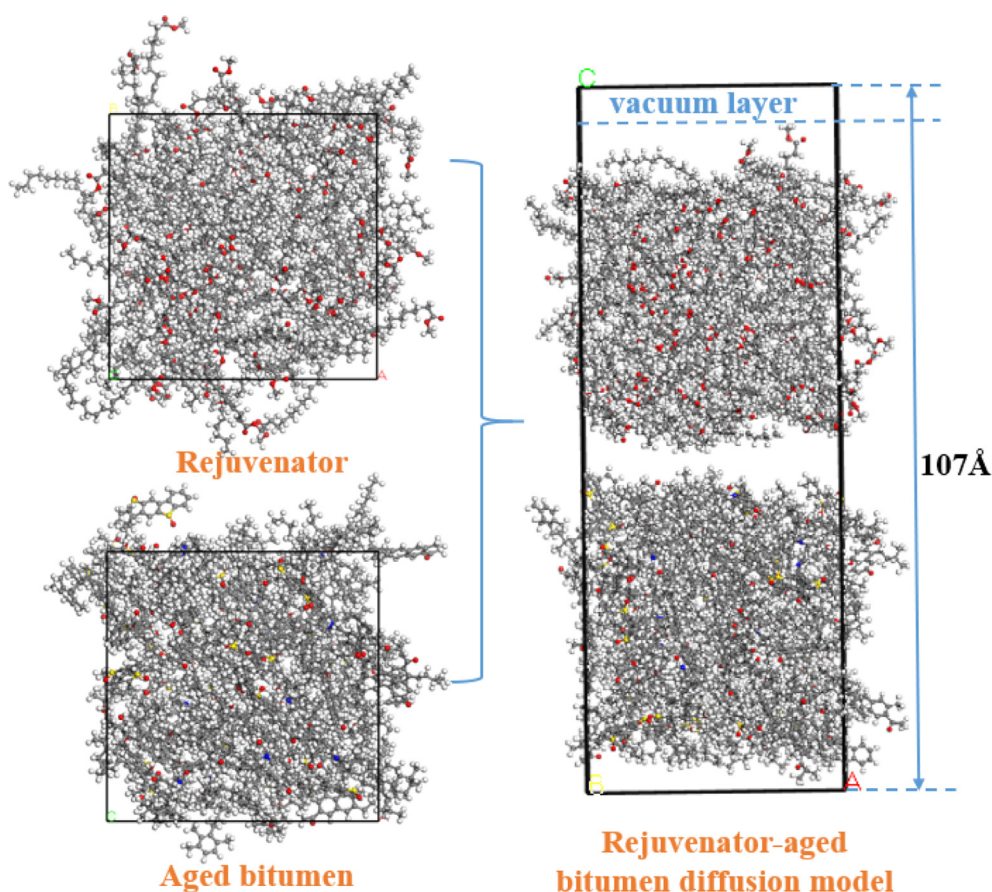


Fig. 5. The rejuvenator-aged bitumen interfacial diffusion molecular model.

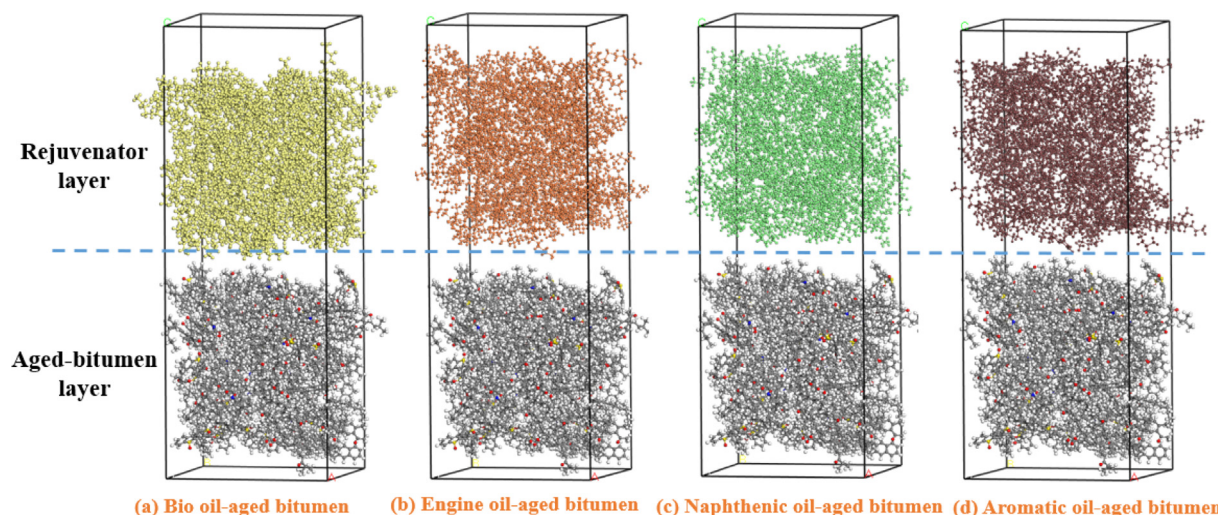


Fig. 6. Different rejuvenator-aged bitumen diffusion molecular models (Yellow: Bio-oil; Orange: Engine-oil; Green: Naphthenic-oil; Brown: Aromatic-oil). (For interpretation of the references to colour in this figure legend, the reader is referred to the web version of this article.)

Table 4
Predicted and measured density values of bitumen and rejuvenator models.

| Density parameter | Predicted values (g/cm ³) | | Measured values (g/cm ³) | |
|-------------------|---------------------------------------|-------|--------------------------------------|-------|
| | 25°C | 60°C | 25°C | 60°C |
| Virgin bitumen | 0.999 | 0.984 | 1.017 | 0.996 |
| Aged bitumen | 1.041 | 1.030 | 1.036 | 1.015 |
| Bio-oil | 0.868 | 0.842 | 0.911 | 0.889 |
| Engine-oil | 0.821 | 0.802 | 0.833 | 0.814 |
| Naphthenic-oil | 0.886 | 0.865 | 0.875 | 0.852 |
| Aromatic-oil | 0.971 | 0.955 | 0.994 | 0.978 |

From **Table 4**, it is demonstrated that the predicted values of virgin bitumen, aged bitumen, and four rejuvenators are close to the experimental results at both 25 °C and 60 °C. It strongly validates the reasonability of established molecular models of aged bitumen and rejuvenators. The density of aged bitumen is larger than virgin bitumen due to the increment in the asphaltene/maltene ratio and the involvement of polar functional groups. All rejuvenators exhibit a lower density than virgin and aged bitumen, which manifests their rejuvenation potential in restoring the density values of aged bitumen to the virgin bitumen level. The aromatic-oil rejuvenator shows the highest density, followed by the bio-oil and naphthenic-oil, while the engine-oil exhibits the lowest density. It is worth noting that there is still a little difference between the predicted and measured values. The reason may be that the utilization of one average molecular model to represent the rejuvenator molecules would ignore the realistic chemical components of bitumen and rejuvenators composed of lots of low and high molecular-weight molecules, which plays an essential role in determining their physical and thermodynamic properties [47].

4.5. Basic theory

The diffusion behavior is a material transfer process from a high-concentration region to another low-concentration phase until attaching an equilibrium state, which is characterized by a concentration gradient index [48]. Fick's Second Law generally describes the interdiffusion behavior and quantitatively derives

the diffusion rate between different materials phases, assuming no volume change during a diffusion process.

$$\frac{\partial c}{\partial t} = \frac{\partial}{\partial z} \left(D(c) \cdot \frac{\partial c}{\partial z} \right) \quad (3)$$

where c refers to a mass concentration, g/cm³; t is the diffusion time, ns; z represents a position point, Å; and $D(c)$ is an interfacial diffusion coefficient, m²/s.

From **Eq. 3**, it can be seen that the diffusion coefficient parameter $D(c)$ is related to concentration C . To simplify, we assume that the $D(c)$ is independent of the concentration C and keeps a constant value of D_0 during the whole diffusion procedure. Fick's Second Law can be expressed as a function of diffusion time t and position z , as presented in **Eq. 4**.

$$c(z, t) = c_0 \left(1 - \operatorname{erf} \left(\frac{z}{2\sqrt{D_0 t}} \right) \right) \quad (4)$$

where $c(z, t)$ is the concentration distribution of diffusive substances (rejuvenator molecules); c_0 represents the equilibrium rejuvenator concentration; erf is an error function, and D_0 is the constant interdiffusion coefficient, m²/s. Moreover, t and z show the diffusion time (ns) and a position point (Å).

5. MD simulation results and discussion

5.1. Molecular configurations of interfacial diffusion models

The molecular configurations of different rejuvenator-aged bitumen diffusion models at the diffusion times of 0, 2, 4, 8, and

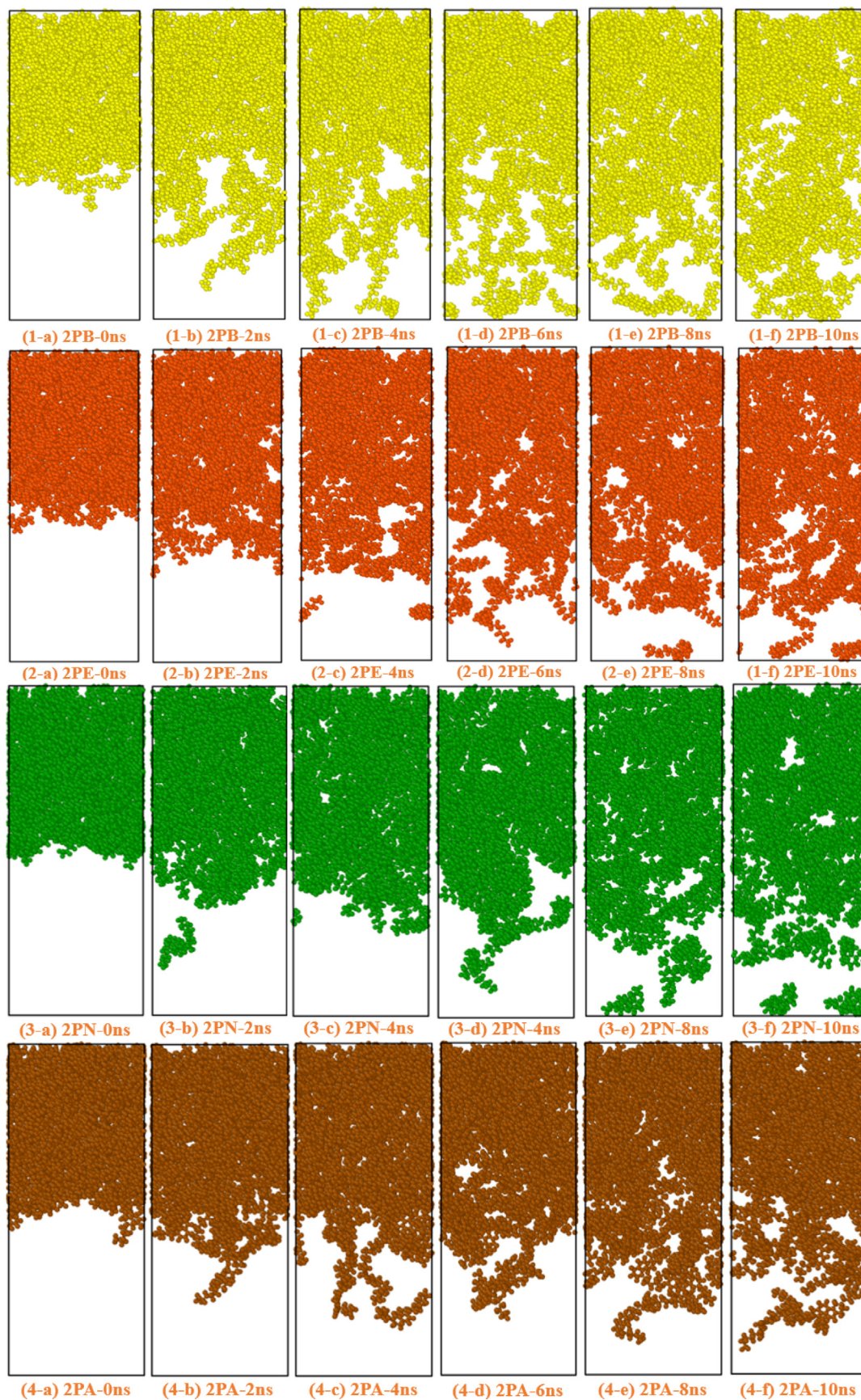


Fig. 7. The snapshots of rejuvenator-aged bitumen models after MD diffusion simulations at 160°C (Bio-oil: Yellow; Engine-oil: Red; Naphthenic-oil: Green; Aromatic-oil: Brown). (For interpretation of the references to colour in this figure legend, the reader is referred to the web version of this article.)

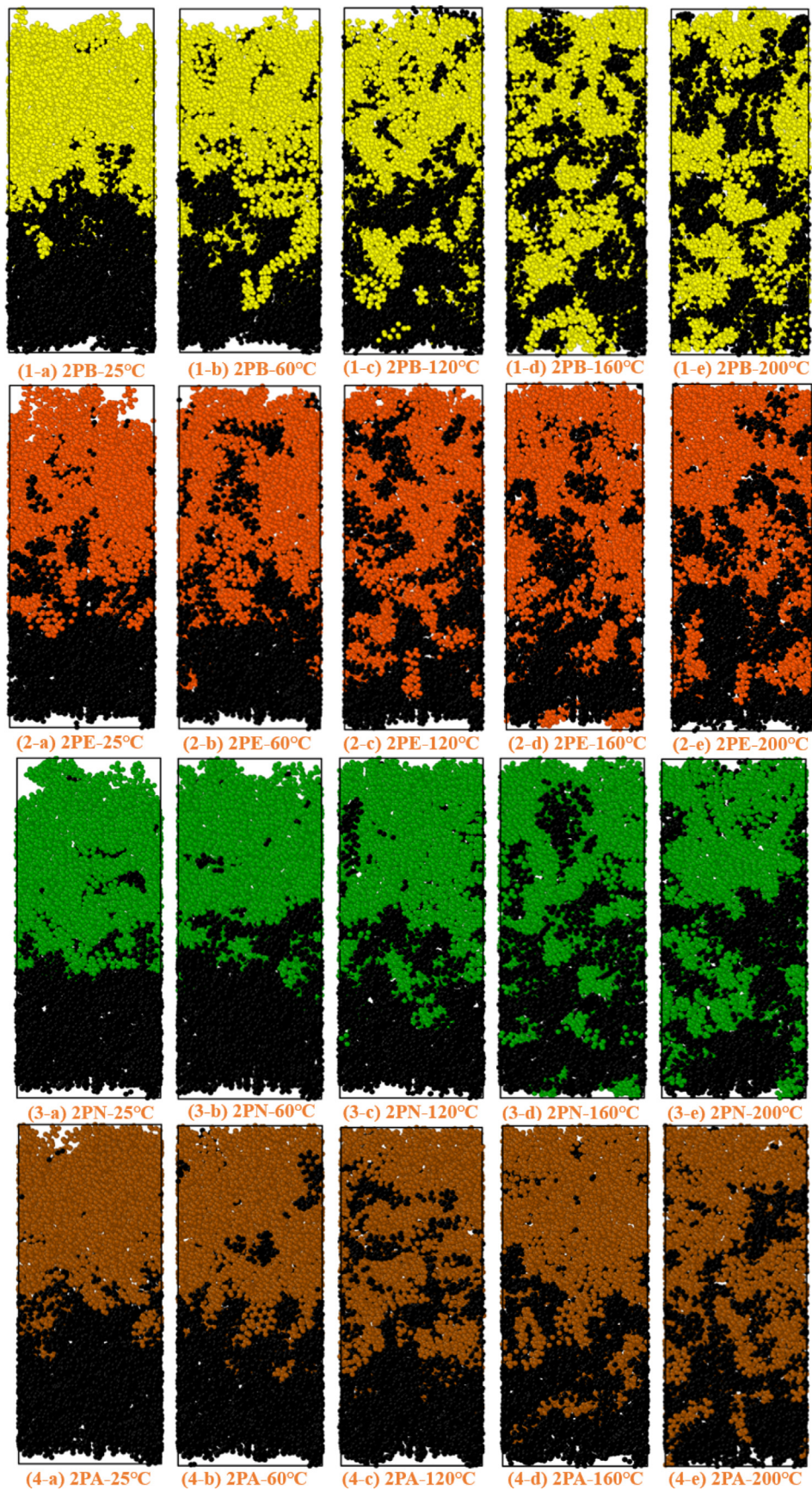


Fig. 8. The snapshots of rejuvenator-aged bitumen molecular models at different temperatures at 10 ns (Bio-oil: Yellow; Engine-oil: Red; Naphthenic-oil: Green; Aromatic-oil: Brown; Bitumen: Black). (For interpretation of the references to colour in this figure legend, the reader is referred to the web version of this article.)

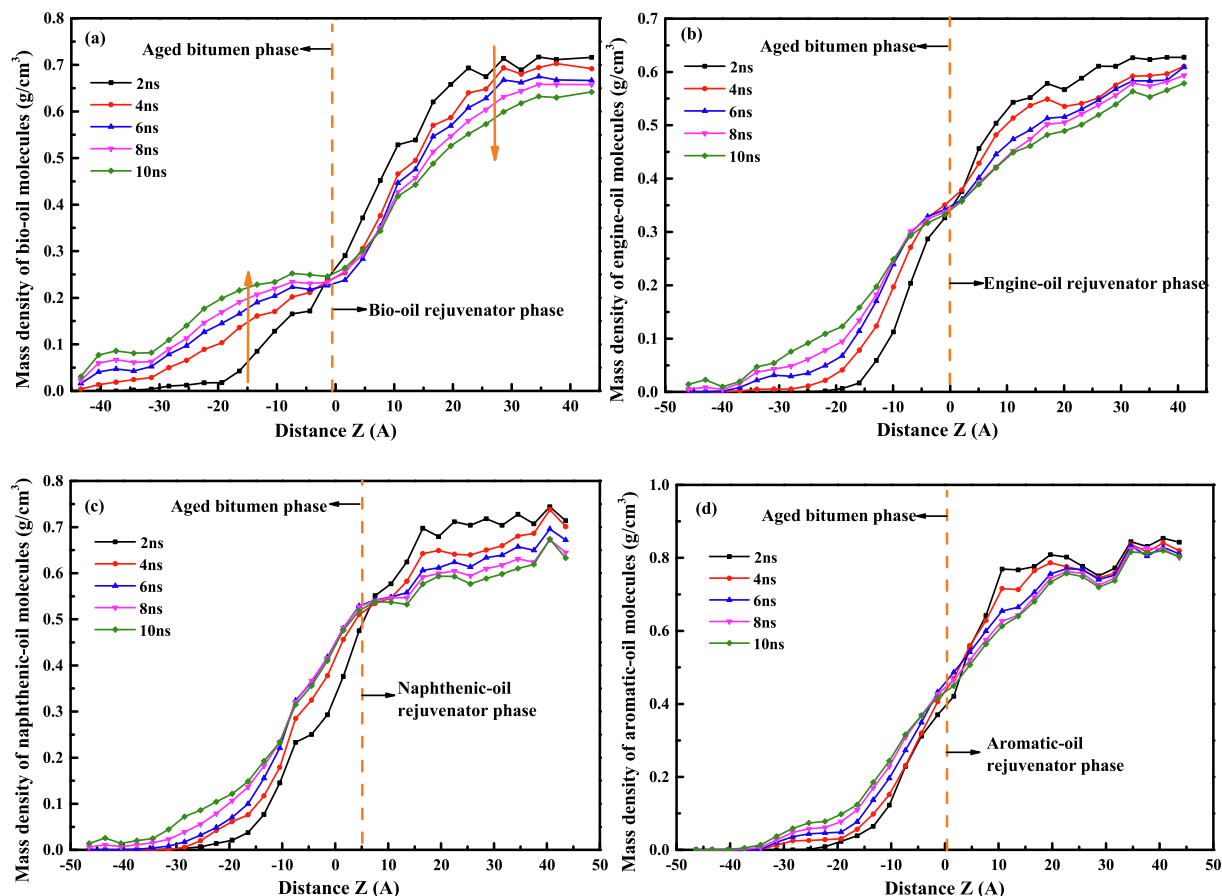


Fig. 9. Mass density profile of rejuvenators in bi-layer systems (a) Bio-oil; (b) Engine-oil; (c) Naphthenic-oil; (d) Aromatic-oil.

10 ns are illustrated in Fig. 7. Here only displays the conformations at 160°C, and bitumen molecules are concealed to monitor the diffusion trajectories of rejuvenator molecules clearly. As the diffusion time prolongs, all rejuvenator molecules gradually diffuse into the aged bitumen layer. When the diffusion time is at 10 ns, part of the rejuvenator molecules could reach the bottom of the aged bitumen layer. However, the diffusion time of 10 ns is still insufficient to form a homogenous rejuvenated bitumen, which agrees well with the previous finding that the partial blending between rejuvenator and aged bitumen was observed during the recycling of asphalt mixtures [5,20]. In addition, the micro-voids in a rejuvenator layer refer to the bitumen molecules, indicating that the interfacial diffusion phenomenon between the rejuvenator and aged bitumen molecules is mutual, which was also observed by microscopic morphologies [16,17].

Interestingly, no aromatic-oil molecule compasses to the underside of the aged bitumen layer even though the diffusion time is at 10 ns. It implies that the diffusion rate of aromatic-oil molecules is the lowest among these four rejuvenators, which is related to its highest molecular weight, polarity, and intermolecular interaction with aged bitumen molecules [45]. Moreover, the amount of aged bitumen molecules in the aromatic-oil layer is the least; thus, a long blending time is required to obtain a homogeneous aromatic-oil rejuvenated bitumen. On the contrary, the bio-oil molecules can reach the bottom surface of the aged bitumen layer at 4 ns, and the corresponding molecular amount at 10 ns is the largest. Therefore, it suggests that the bio-oil molecules exhibit the highest diffusion capacity in aged bitumen, which may be associated with its lowest molecular weight and strongest molecular

mobility characteristics [39]. In addition, the diffusion levels of engine-oil and naphthenic-oil molecules are in the middle, while the former displays a greater diffusion rate than the latter. In summary, when the diffusion time and temperature are fixed, the magnitude of the molecular concentration for four rejuvenators in aged bitumen is $BO > EO > NO > AO$.

To predict and explore the temperature influence on diffusion behaviors of rejuvenators in aged bitumen at an atomic scale, the molecular configurations of four rejuvenators at 10 ns and different diffusion temperatures of 25, 60, 120, 160, and 200°C. The representative results are illustrated in Fig. 8. The rejuvenator and aged bitumen molecules are displayed herein to observe the intermolecular diffusion and distribution level. All rejuvenator molecules show a deeper penetrating trend when the temperature increases, denoting that a high temperature promotes the diffusion rate of rejuvenator molecules. At the same time, more bitumen molecules penetrate the rejuvenator layer at high temperatures. However, at both 25 and 60°C, the amount of rejuvenator molecules in the aged bitumen layer is minimal, especially for the engine-oil, naphthenic-oil, and aromatic-oil rejuvenators. The diffusion temperature should be higher than 120°C to ensure a high blending degree between the rejuvenator and aged bitumen within a short mixing period.

On the other hand, the diffusion behavior of rejuvenator molecules in aged bitumen strongly depends on the rejuvenator type and component. At all simulation temperatures, the penetrating levels of bio-oil and aromatic-oil molecules are the largest and smallest, respectively. More engine-oil molecules penetrate aged bitumen layer than the naphthenic-oil rejuvenator. It means

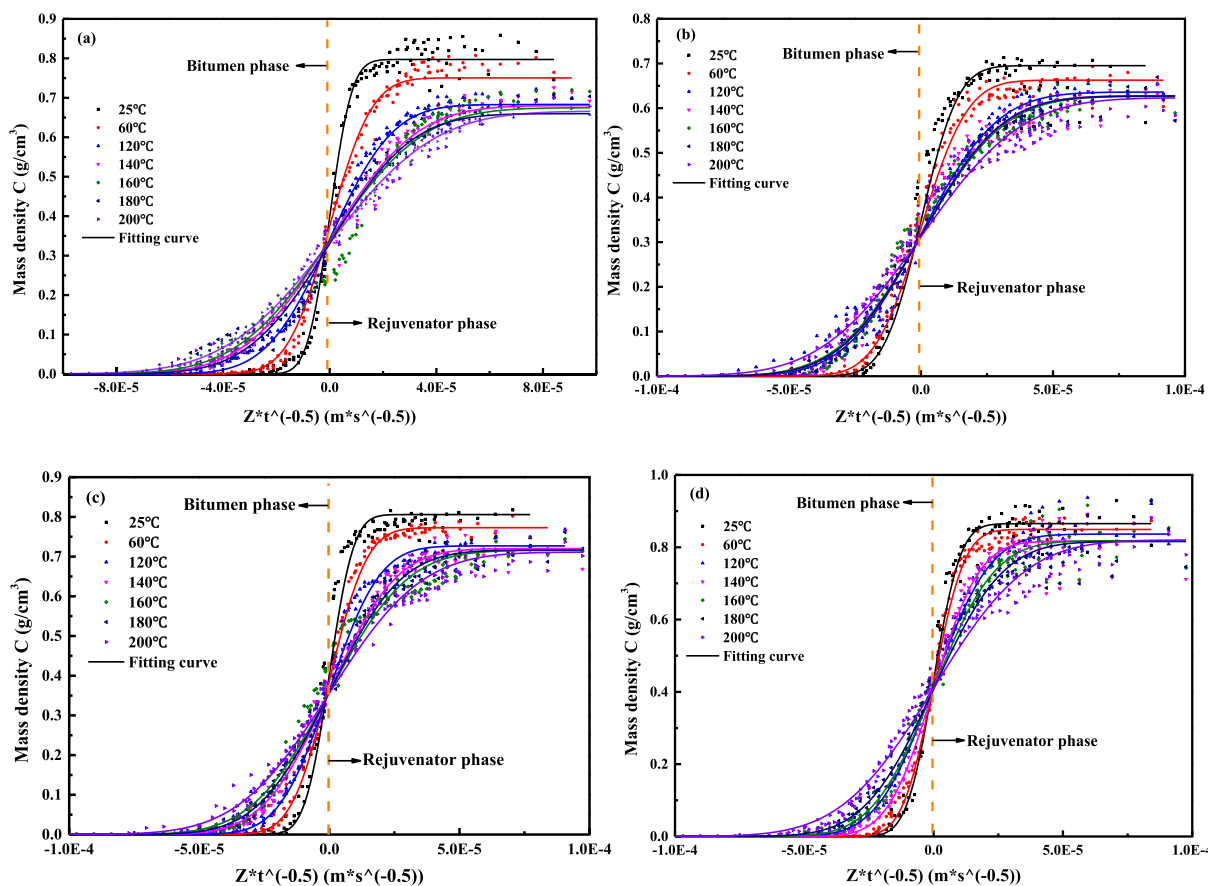


Fig. 10. Density profiles for rejuvenator molecules scaled with $zt^{-0.5}$ in aged bitumen (a) Bio-oil; (b) Engine-oil; (c) Naphthenic-oil; (d) Aromatic-oil.

Table 5
The parameters in fitting curves of different rejuvenator-aged bitumen models.

| Model | T (°C) | -b | C ₀ (g·cm ³) | R ² | Model | -b | C ₀ (g·cm ³) | R ² |
|---|--------|---------|-------------------------------------|----------------|---|--------|-------------------------------------|----------------|
| (a) BO and Aged bitumen system | 25 | 107,414 | 0.399 | 0.995 | (b) EO and Aged bitumen system | 61,202 | 0.355 | 0.988 |
| | 60 | 55,692 | 0.378 | 0.995 | | 50,911 | 0.331 | 0.988 |
| | 120 | 37,954 | 0.342 | 0.994 | | 38,065 | 0.318 | 0.986 |
| | 140 | 27,609 | 0.340 | 0.992 | | 29,465 | 0.314 | 0.986 |
| | 160 | 25,585 | 0.337 | 0.974 | | 28,551 | 0.313 | 0.987 |
| | 180 | 24,133 | 0.330 | 0.983 | | 25,767 | 0.314 | 0.995 |
| | 200 | 22,648 | 0.333 | 0.993 | | 23,638 | 0.312 | 0.976 |
| (c) NO and aged bitumen system | 25 | 96,059 | 0.403 | 0.987 | (d) AO and aged bitumen system | 86,351 | 0.433 | 0.993 |
| | 60 | 62,323 | 0.386 | 0.995 | | 74,818 | 0.425 | 0.996 |
| | 120 | 46,346 | 0.363 | 0.992 | | 48,172 | 0.418 | 0.994 |
| | 140 | 35,102 | 0.360 | 0.994 | | 45,471 | 0.408 | 0.993 |
| | 160 | 29,983 | 0.358 | 0.979 | | 37,847 | 0.409 | 0.989 |
| 180 | 27,387 | 0.358 | 0.994 | 33,390 | 0.408 | 0.988 | | |
| 200 | 25,328 | 0.356 | 0.987 | 25,023 | 0.410 | 0.986 | | |

that the penetrating capacity of engine-oil molecules is more substantial than naphthenic-oil. The molecular distribution of rejuvenators in aged bitumen varies remarkably after an MD diffusion simulation. Compared to other rejuvenators, bio-oil molecules are dispersed more homogeneously in aged bitumen, especially at 200°C. However, it should be mentioned that the molecular-scale distribution of rejuvenators in aged bitumen is still heterogeneous, even though the rejuvenator molecules are entirely blended in aged bitumen. At the same time, the agglomeration phe-

nomenon of rejuvenator molecules is still apparent. In addition, the partial diffusion characteristic of engine-oil, naphthenic-oil, and aromatic-oil molecules in aged bitumen are observed at all temperatures. It indicates that the diffusion time of 10 ns is insufficient for these rejuvenator molecules to diffuse in the aged bitumen layer entirely due to a low diffusion rate. In view of these molecular conformations, the diffusion capacities of bio-oil and engine-oil molecules are more significant than the naphthenic-oil and aromatic-oil rejuvenators.

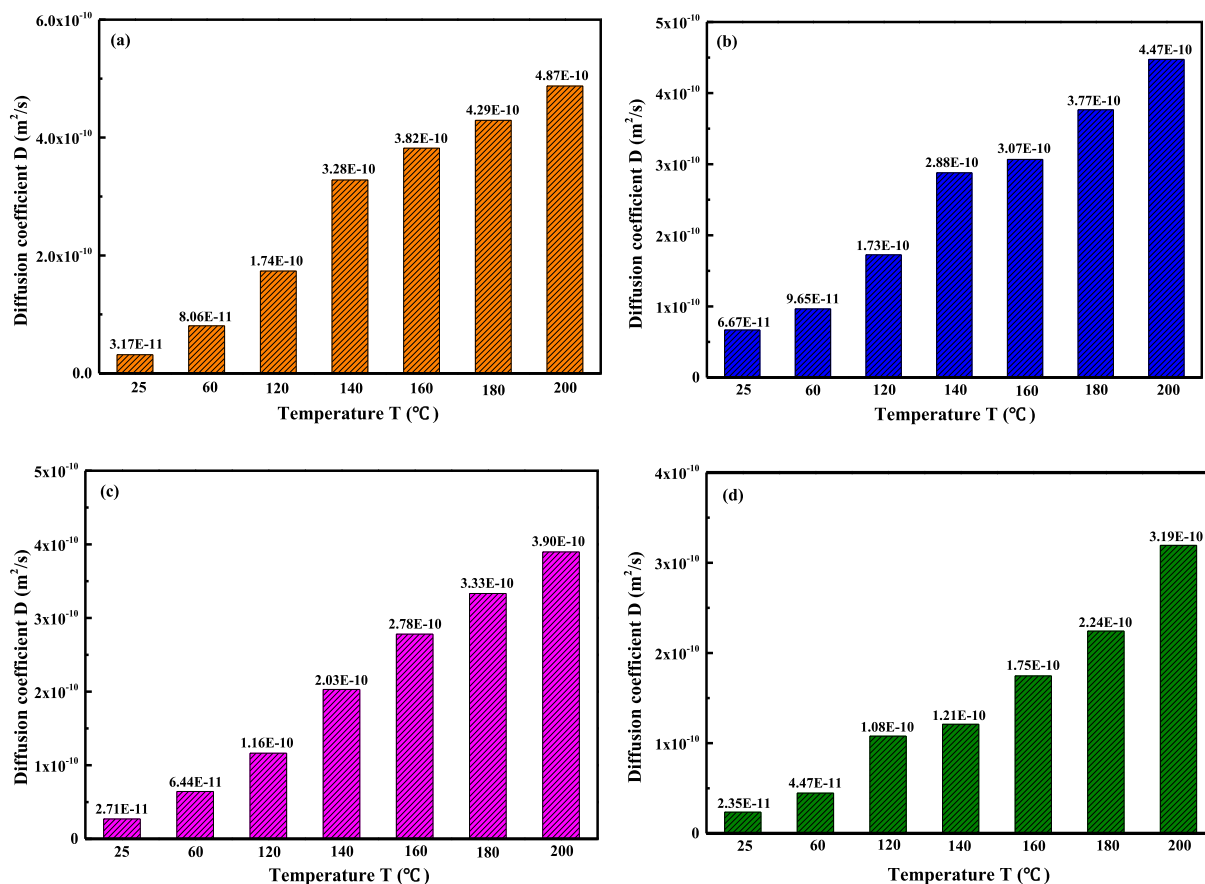


Fig. 11. Diffusion coefficient of rejuvenators in aged bitumen versus temperatures (a) Bio-oil; (b) Engine-oil; (c) Naphthenic-oil; (d) Aromatic-oil.

5.2. Mass density distribution of rejuvenators

The mass density distribution of rejuvenator molecules in aged bitumen is monitored as a function of the diffusion time. The mass density curves of different rejuvenators at 160°C with variable diffusion times of 2, 4, 6, 8, and 10 ns are extracted and drawn in Fig. 9. For simplicity, these corresponding results at different temperatures of 25, 60, 120, 140, 180, and 200°C are not displayed herein. The mass density values of rejuvenator molecules in a rejuvenator phase are much higher than that in the aged bitumen phase, regardless of the rejuvenator type and diffusion duration. It implies that the diffusive equilibrium points of these rejuvenator-aged bitumen models have not been reached yet because of insufficient simulation time. Moreover, the mass density of rejuvenator molecules in the rejuvenator layer is not constant and decreases as the distance to the interface reduces. It reveals that the interfacial diffusion behavior of a rejuvenator-aged bitumen layer is bidirectional, and several bitumen molecules also diffuse into the rejuvenator layer. In the aged bitumen layer, the mass density of rejuvenator molecules shows a decreasing trend as the distance from the interface increases. It means that the distribution of diffused rejuvenator molecules in aged bitumen is stepped, which can be observed from the snapshots of molecular diffusion models in Fig. 7 and Fig. 8.

In addition, the mass density of the rejuvenator molecules in the aged bitumen phase gradually increases with increasing diffusion time while the mass density in the rejuvenator phase decreases. It implies that the increment in diffusion time enlarges the blending level between the rejuvenator and aged bitumen

molecules, which agrees well with the reported experimental results in previous studies [49,50]. When the aging degree of bitumen and diffusion time are fixed, the mass curves of rejuvenator molecules in aged bitumen matrix depend on the rejuvenator type. It is associated with the difference in diffusion capacity and density between these four rejuvenators.

5.3. Correlation curves between mass density and $Z^*t^{-0.5}$

The diffusion coefficient parameters of four rejuvenators in aged bitumen at different temperatures are calculated according to Fick's Second Law (see Eq. 4), and the correlation curves between mass density and $(z/t^{0.5})$ parameter are summarized in Fig. 10. When the diffusion time and depth are the same, the mass density values of rejuvenator molecules in the aged bitumen phase significantly enlarge as the temperature rises, which decreases correspondingly in the rejuvenator layer due to the reduction in rejuvenator molecular amount and increase in bitumen molecules. It is consistent with the previous finding that a high temperature is beneficial to accelerate the blending degree between rejuvenators and aged bitumen in reclaimed asphalt pavement (RAP) materials [51].

Eq. 4 is utilized to fit the correlation curves between the mass density C of rejuvenator molecules and the $(z^*t^{-0.5})$ parameter, and these fitting curves are also displayed in Fig. 10. Meanwhile, all related fitting parameters are listed in Table 5. According to R^2 values higher than 0.97, the fitting efficiency of Fick's Second Law on diffusion characteristics of all rejuvenators is satisfactory. The parameter C_0 represents the initial concentration of rejuvena-

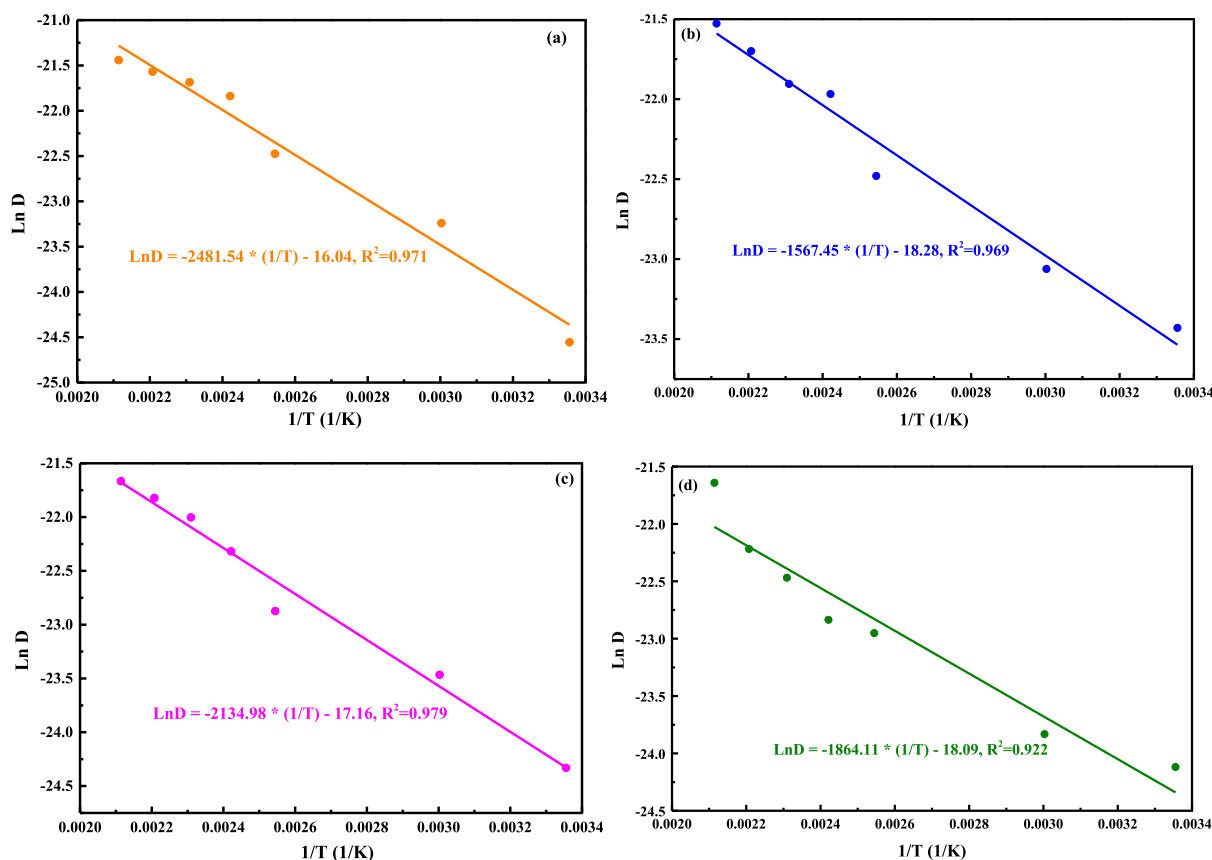


Fig. 12. Correlations between temperature and diffusion coefficient of rejuvenators in aged bitumen.

Table 6

The E_a and A parameters of various rejuvenators in LAB40-aged bitumen.

| Rejuvenator | BO | EO | NO | AO |
|-----------------|----------|----------|----------|----------|
| E_a (J/mol) | 18968.72 | 15256.02 | 13030.91 | 15498.21 |
| A (m^2/s) | 1.08E-7 | 1.15E-8 | 3.52E-8 | 1.39E-8 |

tor molecules in the bulk rejuvenator phase. The C_0 values of all rejuvenators have a reduction trend as the temperature increasing, which is attributed to the decreased density of rejuvenators at high temperatures. When the temperature is at the same level, the magnitude of C_0 values for four rejuvenators is $AO > NO > BO > EO$. Moreover, parameter b ($b = 1/(2 * D^{0.5})$) shows a negative relationship with the diffusion coefficient (D) values of rejuvenators. With the diffusion temperature rising, the b values in these correlation curves decrease, particularly when the temperature rises from 25°C to 60°C. It denotes that the diffusion rates of rejuvenators in aged bitumen enlarge distinctly at high temperatures.

5.4. Diffusion coefficient prediction of different rejuvenators in aged bitumen

To directly evaluate and compare the diffusion capacity of various rejuvenators in aged bitumen at different temperatures, the diffusion coefficient (D) values are calculated and plotted in Fig. 11. It can be seen that the magnitude for D parameters of four rejuvenators varies from 10^{-11} to 10^{-10} m^2/s , which depends on both rejuvenator type and temperature dramatically. All D values of rejuvenators enlarge remarkably as the diffusion temperature

rises. On the one hand, the enhanced molecular mobility of rejuvenator molecules at high temperatures would promote the permeation level of rejuvenators into the aged bitumen layer [28,29]. On the other hand, the increased temperature would enlarge the free volume ratio in aged bitumen and create more spatial volume for further diffusion of rejuvenator molecules [27]. The aromatic-oil rejuvenator exhibits the lowest diffusion coefficient D value in the whole diffusion temperature region. Polar aromatic rings strongly reduce the molecular mobility of aromatic-oil molecules. In the meantime, the energetical intermolecular interaction between aromatic-oil and aged bitumen molecules would hinder its deep penetration.

In addition, the D values of bio-oil and engine-oil rejuvenators are more significant than the naphthenic-oil. This is because the high molecular weight characteristic of the naphthenic-oil molecule negatively affects its molecular mobility. Interestingly, the comparison results regarding the diffusion coefficient values of bio-oil and engine-oil rejuvenators depend on the diffusion temperature. At low temperatures (25°C and 60°C), the engine-oil rejuvenator displays higher D values than the bio-oil, while the latter shows the largest diffusion coefficient at high temperatures (120–200°C). The diffusion process of rejuvenator molecules in the aged

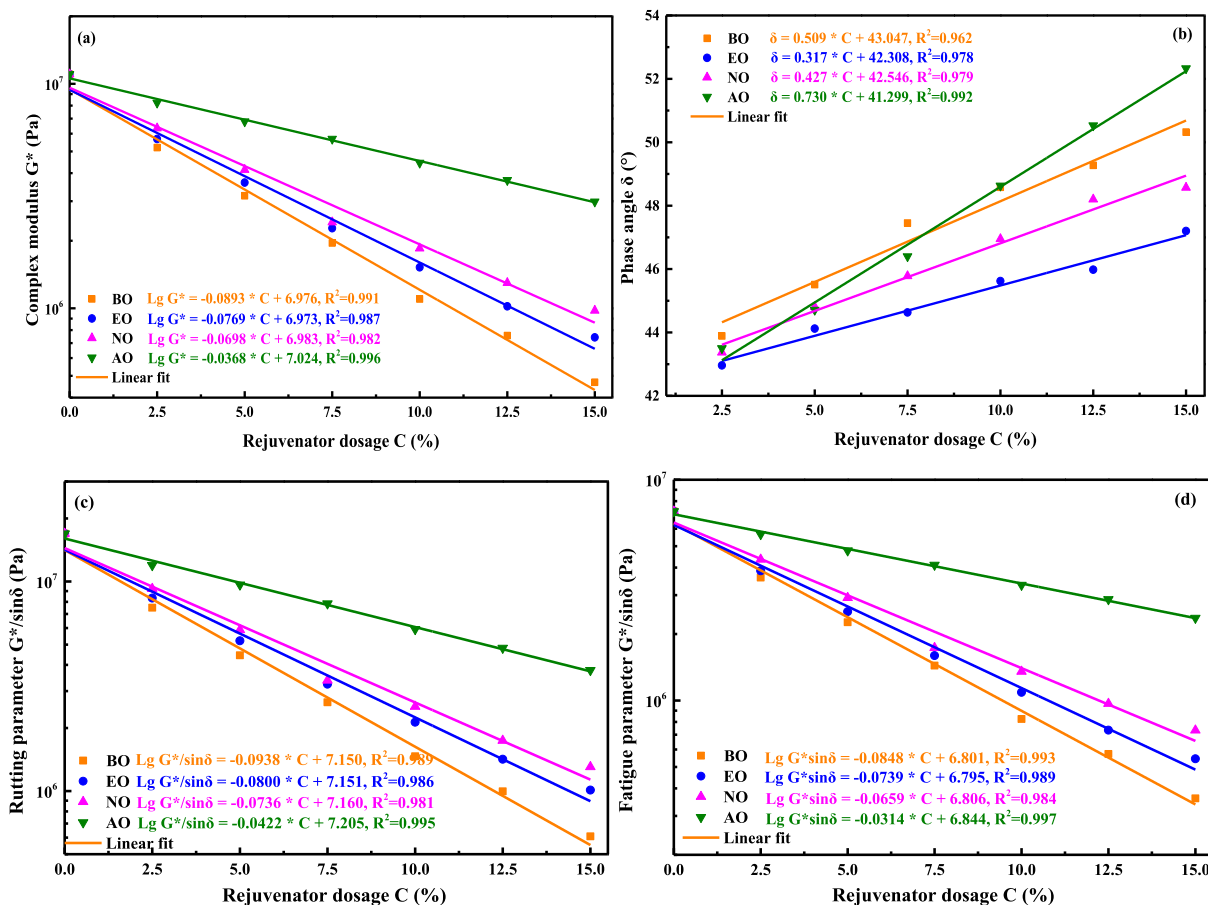


Fig. 13. Correlation curves between different rheological indices at 20°C and 0.1 rad/s with rejuvenator dosage.

bitumen layer is complicated. Meanwhile, the diffusion rate is associated with the molecular mobility of rejuvenator molecules and the intermolecular interaction with aged bitumen molecules. At low temperatures, a polar ester functional group in bio-oil molecules improves the intermolecular interaction with aged bitumen molecules, which blocks the diffusion potential of bio-oil molecules due to insufficient molecular mobility. As a result, the intermolecular interactions between engine-oil and aged bitumen molecules are much lower than bio-oil, and that's why the engine-oil molecules exhibit a higher diffusion coefficient than the bio-oil at low temperatures. However, bio-oil molecules' molecular mobility and self-diffusion capacity are more significant than the engine-oil molecules at high temperatures, as reported in our previous work [45]. Therefore, the bio-oil rejuvenator shows a faster diffusion rate than the engine-oil at high temperatures.

It is summarized that the rejuvenator type significantly influences the diffusion capacity of rejuvenators in aged bitumen. For instance, the D value of engine-oil molecules in aged bitumen at 60°C is 1.20, 1.50, and 2.16 times larger than that of bio-oil, naphthenic-oil, and aromatic-oil rejuvenators. Meanwhile, the D value of bio-oil rejuvenator at 160°C is 1.24, 1.37, and 2.18 times higher than engine-oil, naphthenic-oil, and aromatic-oil molecules. Compared to bio-oil and engine-oil rejuvenators, a higher blending temperature is needed for both naphthenic-oil and aromatic-oil to diffuse and disperse in aged bitumen homogeneously. Furthermore, during the mixing and compaction processes, the bio-oil rejuvenator would diffuse faster than engine-oil due to the high temperature (>120°C), but the latter would show a higher diffusion

capacity than the former when the temperature of recycled asphalt pavement is lower than 60°C.

5.5. Influence of temperature on D values of different rejuvenators in aged bitumen

To further explore the influence of temperature on the diffusion behaviors of various rejuvenators in aged bitumen, the Arrhenius equation is utilized to describe the relationship between the diffusion coefficient and temperature, which is expressed as follows:

$$\ln D = \frac{-E_a}{R} * \frac{1}{T} + \ln A \tag{5}$$

where D is the diffusion coefficient, m²/s; T shows the diffusion temperature, K; R refers to the universal gas constant (8.314 J/mol·K⁻¹), E_a and A represent the activation energy (J/mol) and pre-exponential factor (m²/s). It is worth noting that the E_a parameter is related to the critical energy for rejuvenator molecules to diffuse into aged bitumen layer, while the A parameter herein means the maximum diffusion coefficient point of rejuvenator molecules when the diffusion temperature is to infinity.

Fig. 12 demonstrates the correlation curves between the (LnD) of four rejuvenators and the (1/T) parameter, and the corresponding fitting equations. The correlation coefficient R² values are all higher than 0.90, indicating that the Arrhenius formula could fit the LnD-1/T curves of all rejuvenators well. Moreover, the LnD values present a linear relationship with a reciprocal diffusion temperature. It can be found that the D values of four rejuvenators

exhibit diverse temperature sensitivity. The magnitude of slope values (E_a/R) for four rejuvenators is $BO > AO > EO > NO$. It implies that the diffusion capacity of bio-oil molecules in aged bitumen presents the highest sensitivity to temperature variation, followed by aromatic-oil and engine-oil, while the naphthenic-oil shows less temperature sensitivity. The E_a and A values of four rejuvenators are listed in Table 6. The order of pre-exponential factor (A) and activation energy (E_a) values for four rejuvenators is the same as $BO > NO > AO > EO$. When the temperature tends to the infinity point, the diffusion rate of engine-oil molecules is the smallest, while the bio-oil molecules exhibit the most considerable diffusion potential. In addition, the activation energy required for engine-oil molecular diffusion is the lowest, indicating that it is easiest for engine-oil molecules to have enough molecular mobility to penetrate in aged bitumen layer due to its lower molecular weight and absence of a polar functional group. On the contrary, the E_a value of bio-oil is higher than that of aromatic-oil and engine-oil rejuvenators. Although the bio-oil molecule has the smallest molecular weight and largest molecular mobility, the potential hydrogen bonds between the ester function group ($-COO-$) in bio-oil molecules and hydrogen atoms in bitumen molecules

would hinder the deep diffusion process of bio-oil molecules in aged bitumen, which agrees well with previous findings [29,52].

6. Experimental validations

6.1. Establishing standard curves of rheological indices

In view of the high similarity in physical and chemical characteristics, it is difficult to distinguish the rejuvenator from an aged bitumen matrix. In the previous studies [23,24,53], the variation of rheological indices of aged bitumen layers was measured to monitor the concentration distribution of rejuvenators in aged bitumen after different diffusion tests. To this end, the relationships between the rejuvenator dosage and different rheological indices are determined first in this study. Then, the rejuvenated bitumen with variable rejuvenator types and dosages are manufactured, and their rheological indicators are shown in Figs. 13–15.

The rheological indices of complex modulus G^* , phase angle δ , rutting parameter $G^*/\sin\delta$, and fatigue parameter $G^*\sin\delta$ values of various rejuvenated binders are displayed in Fig. 13. It is found that the $\log(G^*)$, $\log(G^*/\sin\delta)$, and $\log(G^*\sin\delta)$ values of all rejuvenated bitumen show a linearly decreasing trend as an increment in rejuvenator dosage, while the δ values increase gradually. Thus, incorporating these four rejuvenators can restore the stiffness, viscoelastic ratio, rutting resistance, and fatigue resistance properties of aged bitumen to a virgin level. Nevertheless, the influence of rejuvenator content on these rheological indices is significantly dependent on the rejuvenator type and components. When the rejuvenator dosage is the same, the magnitude of G^* , $G^*/\sin\delta$, and $G^*\sin\delta$ for rejuvenated bitumen with four rejuvenators is the same as $AO > NO > EO > BO$. It suggests that the bio-oil rejuvenator exhibits the largest effect on restoring the stiffness, rutting resistance, and fatigue resistance of aged bitumen. On the contrary, the rejuvenation effect of an aromatic-oil rejuvenator is the smallest as a result of its considerable molecular weight, polarity, and viscosity. Further, the rejuvenation efficiency on rheological performance restoration of engine-oil and naphthenic-oil rejuvenators is in the middle, and the former is better than the latter.

The variable rates of these rheological indices of rejuvenated bitumen with four rejuvenators as a function of the rejuvenator dosage differ dramatically. Based on the absolute slope values in correlation equations, the order of rejuvenator dosage dependence level for the G^* , $G^*/\sin\delta$, and $G^*\sin\delta$ parameters of rejuvenated bitumen with four rejuvenators follows $BO > EO > NO > AO$. Meanwhile, the aromatic-oil rejuvenator shows the strongest influence

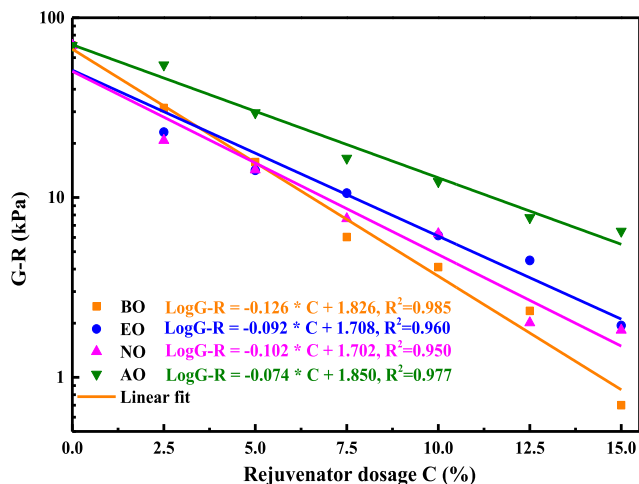


Fig. 14. Correlation curves between the G-R parameter with rejuvenator dosage.

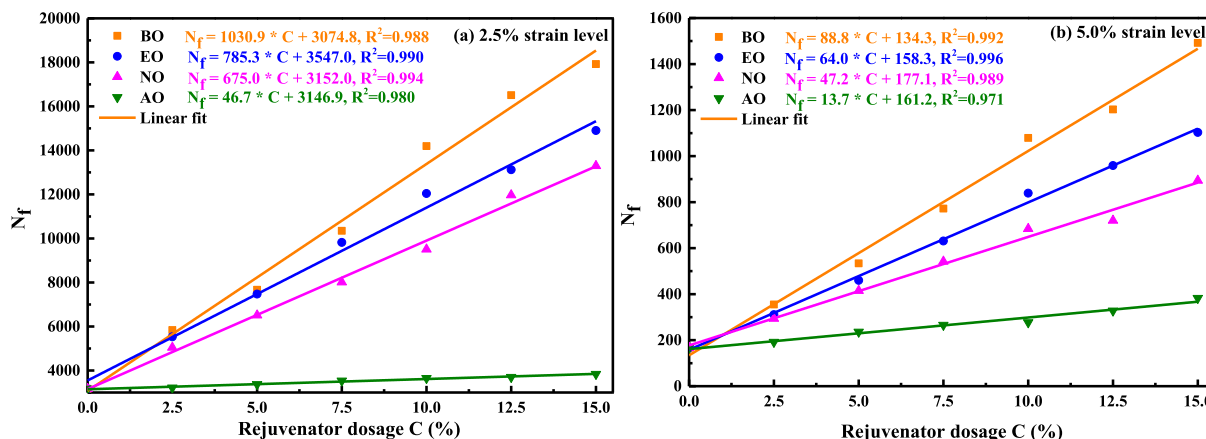


Fig. 15. Correlation curves between the service life N_f with rejuvenator dosage.

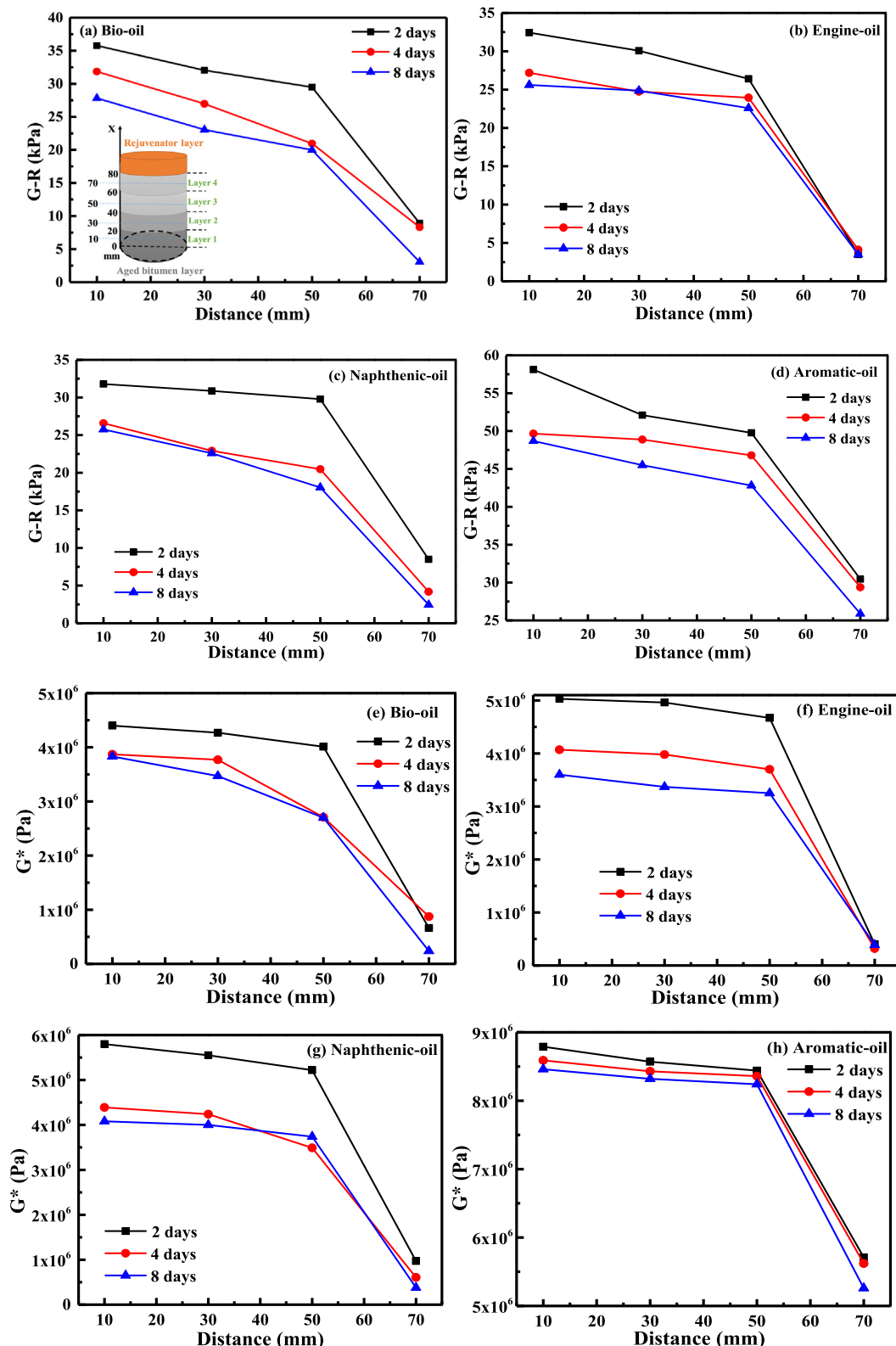


Fig. 16. The $G-R$ (a-d) and G^* (e-h) parameters of rejuvenated bitumen versus diffusion time and position.

on increasing the δ values of aged bitumen, followed by the bio-oil and naphthenic-oil rejuvenators. In contrast, engine-oil rejuvenated bitumen displays the lowest δ values regardless of the reju-

venator dosage. It manifests that an aromatic-oil rejuvenator could maximally restore the viscoelastic ratio of aged bitumen while the influence of engine-oil is the weakest.

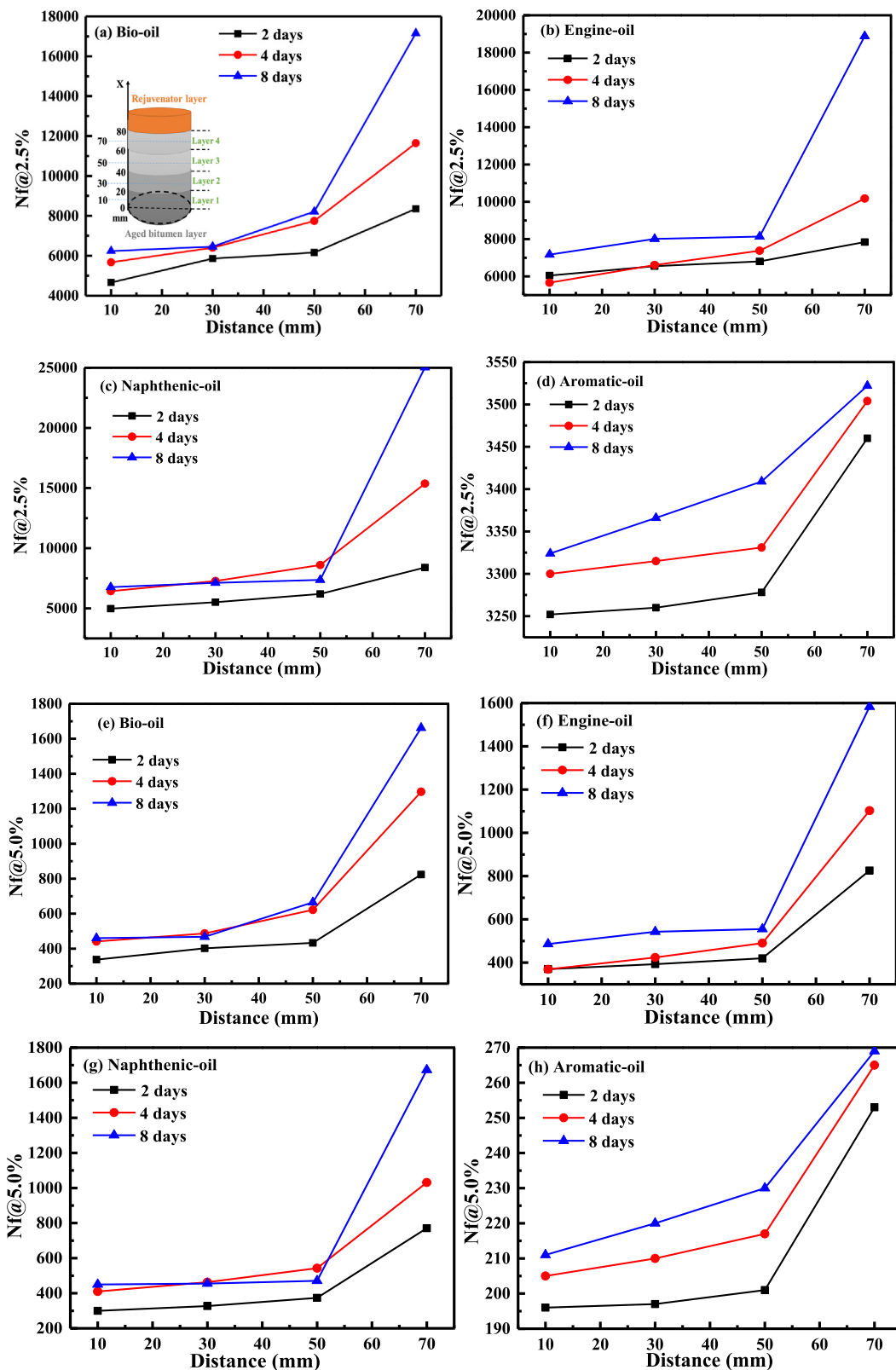


Fig. 17. The $N_f@2.5\%$ (a-d) and $N_f@5.0\%$ (e-h) parameters of rejuvenated bitumen versus diffusion time and position.

Similarly, the correlation curves between the G-R values with the rejuvenator dosage are illustrated in Fig. 14. It was reported that the G-R parameter was strongly associated with the cracking

potential of bitumen, and a high G-R value represented a lower cracking resistance. The aged bitumen exhibits the highest G-R value, which reduces significantly as an increment in rejuvenator

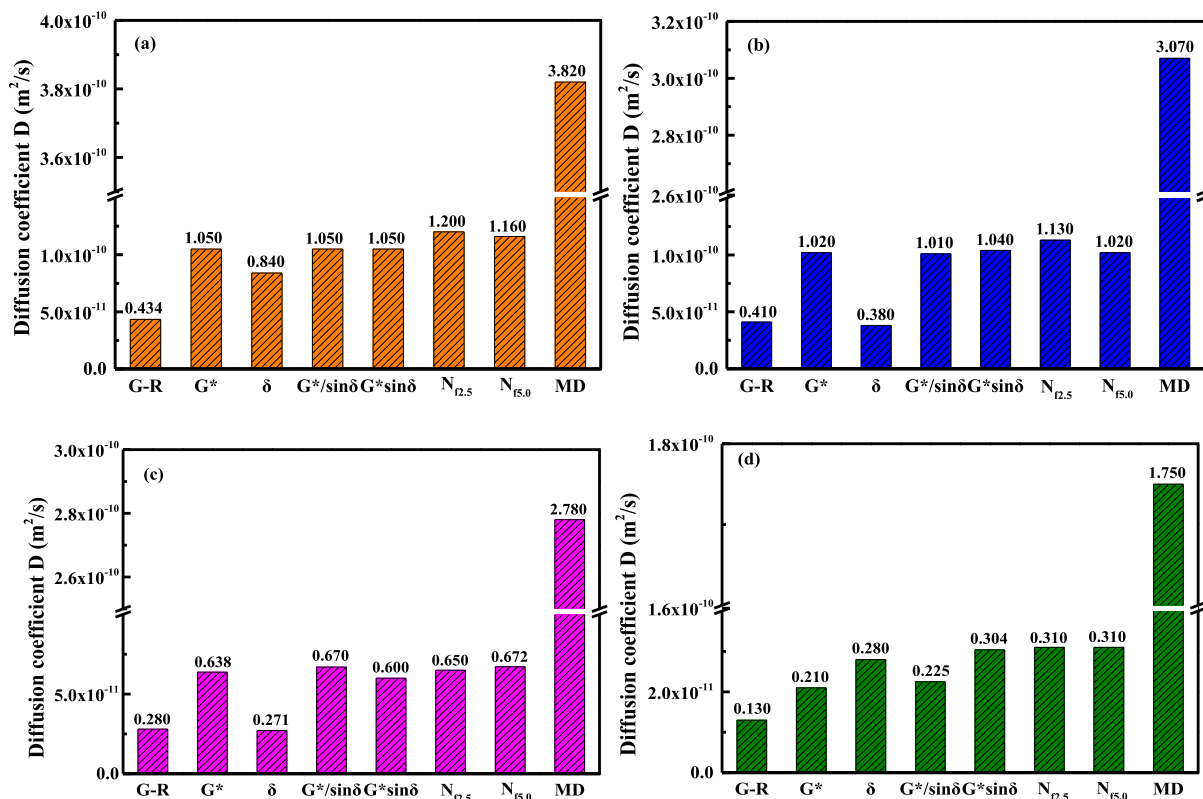


Fig. 18. Comparison of D values from MD outputs and experimental results (a) Bio-oil; (b) Engine-oil; (c) Naphthenic-oil; (d) Aromatic-oil.

content no matter the rejuvenator type. It manifests that involving rejuvenators can distinctly enhance the cracking resistance of aged bitumen. When the rejuvenator dosage is the same, the order of four rejuvenators for an improvement effect on G-R values is BO > EO > NO > AO. Moreover, there is a linear decreasing relationship between the Log (G-R) and C of all rejuvenated binders, and the rejuvenator type presents a significant influence. The G-R parameter of bio-oil and aromatic-oil rejuvenated bitumen displays the most superior and slightest sensitivity to rejuvenator content, while that of engine-oil and naphthenic-oil rejuvenated bitumen are similar and in the middle.

Fig. 15 demonstrates the fatigue life N_f at two strain levels of 2.5 % and 5.0 % of rejuvenated binders with variable rejuvenator dosages. The N_f values of all rejuvenated bitumen increase linearly as rejuvenator content increases. It means that adding these four rejuvenators can enhance the fatigue resistance of aged bitumen. However, the enhancement effect of the aromatic-oil rejuvenator is limited due to its large molecular weight and viscosity [39,45]. The bio-oil rejuvenated binders show the highest N_f values, followed by the engine-oil and naphthenic-oil rejuvenated bitumen. The influence of rejuvenator content on the N_f values is more significant at a lower fatigue strain, which also relies on rejuvenator components. The correlation equation between the N_f and rejuvenator content is utilized to determine the rejuvenator concentration distribution in various diffusion systems and calculate the corresponding diffusion coefficient values of different rejuvenators in aged bitumen.

6.2. Variations of different rheological indices during the diffusion process of various rejuvenators

The diffused samples are equally divided into four parts, and each of them is subjected to rheological tests to determine the con-

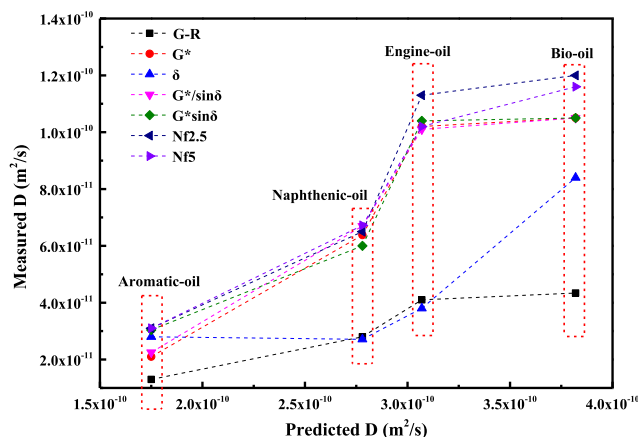


Fig. 19. Influence of rejuvenator type on the diffusion coefficient values.

centration distributions of rejuvenators in diffused specimens. Here only displays the G-R, G^* , and N_f values of bitumen specimens with variable distances and diffusion times, while the results in δ , $G^*/\sin\delta$, and $G^*\sin\delta$ parameters are shown in the “Supplementary materials” section.

Fig. 16 demonstrates the G-R and G^* values of four rejuvenator-aged bitumen diffusion systems as a function of diffusion distance and time. A high distance value denotes that the measured fragment sample is closer to the diffusion interface between the rejuvenator and aged bitumen. From Fig. 16a-d, the G-R values of all

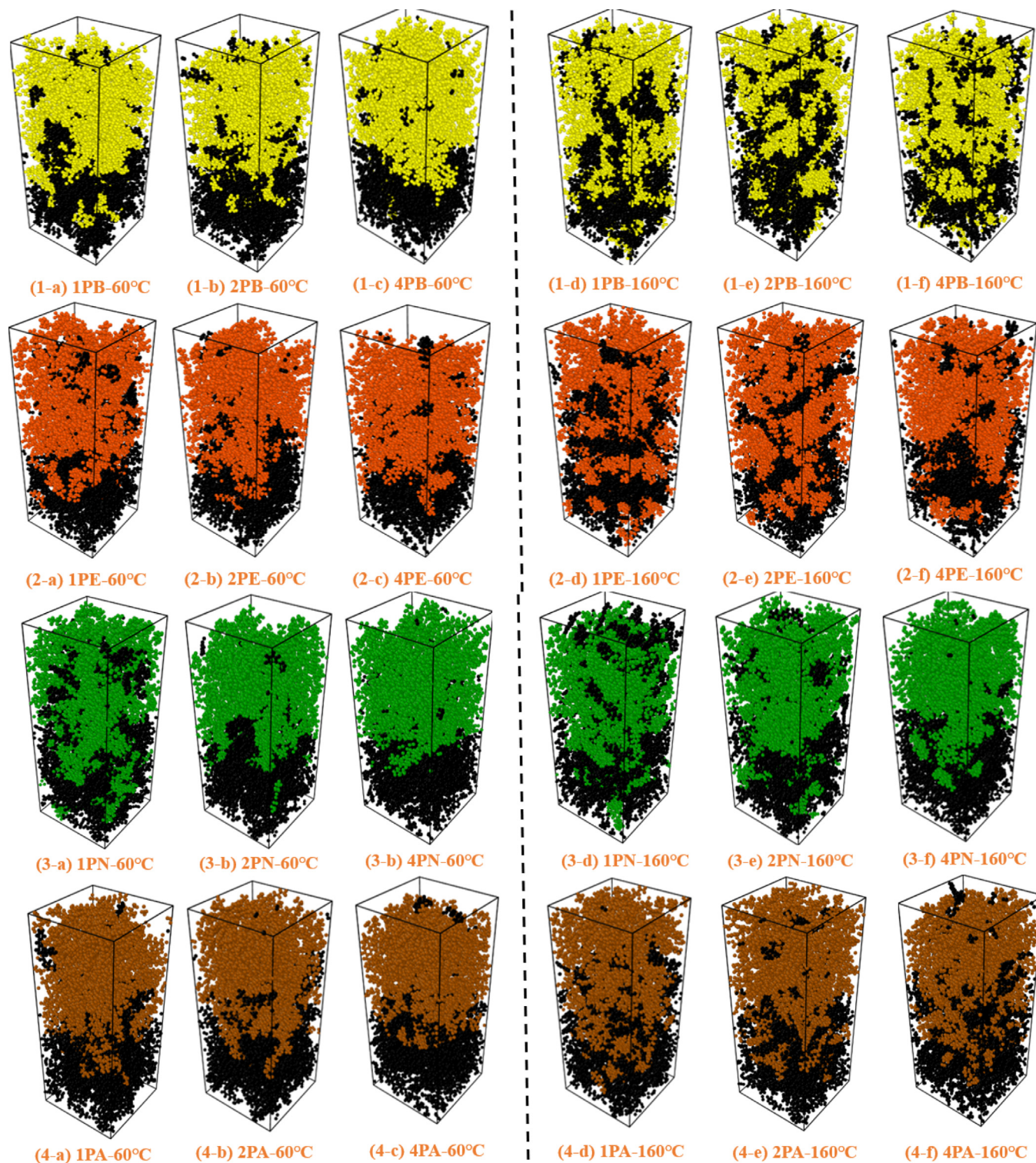


Fig. 20. Molecular configurations of diffusion models with different rejuvenator types and aging degrees at 10 ns (Bio-oil: Yellow; Engine-oil: Red; Napthenic-oil: Green; Aromatic-oil: Brown; Bitumen: Black). (For interpretation of the references to colour in this figure legend, the reader is referred to the web version of this article.)

rejuvenated binders show a reduction trend as an increment in the distance. A lower G-R value refers to a higher rejuvenator dosage in the fragment specimen. It implies that the rejuvenator concentration in the aged bitumen layer increases gradually as the distance extends from the bottom end of the aged bitumen to the interface point. The phenomenon is in good agreement with molecular con-

formations observed from MD simulations. Further, it can be seen that the G-R values at the distance of 70 mm are much lower than other three data points, indicating that the diffusion behaviors of rejuvenators mainly occur in the first layer with a 20 mm thickness adjacent to the interface because of a limited diffusion time. As diffusion time prolongs, the G-R values of diffused specimens at dif-

ferent positions tend to decrease, denoting that the rejuvenator penetrates more and deeper in the aged bitumen layer, which is also consistent with the MD simulation configurations. Meanwhile, the influence of diffusion time on the concentration variation of the rejuvenator in the aged bitumen layer is not constant, and it seems that the diffusion rate of the rejuvenator shows a reduction trend as the diffusion duration extends. This phenomenon was also reported in previous research [24].

Fig. 16e-h illustrate the complex modulus (G^*) distributions of diffused samples at different positions with diffusion times varying. Similar to the G-R parameter, the G^* values decrease as the distance increases. Notably, various rejuvenators exhibit different G^* distributions in diffused specimens. Compared to other rejuvenators, the difference in G^* of AO-aged bitumen diffused specimens at different positions is much more limited. In other words, the influence of diffusion time on the G^* parameter of AO diffusion in aged bitumen is the smallest. It implies that the diffusion capacity of the aromatic-oil rejuvenator is the lowest. Moreover, the G^* variation as a function of diffusion time for the engine-oil diffusion system is more significant than the bio-oil and naphthenic-oil rejuvenators.

Fig. 17 shows the N_f values of different diffused specimens at 2.5 % and 5.0 % strain levels. For all rejuvenators, the diffusion phenomenon mainly occurs at a limited distance (within 20 mm of the interface) because of insufficient diffusion time. It indicates that the diffusion rate of rejuvenators in aged bitumen is andante. As the distance and diffusion time increase, the N_f values of rejuvenator-aged bitumen diffused specimens enlarge, showing

that the diffusion degrees of all rejuvenators in aged bitumen increase with an increment of diffusion duration. However, various rejuvenators present different diffusion degrees when the diffusion temperature, position, and time keep constant.

6.3. Comparison of the diffusion coefficient values of rejuvenators

In this study, the diffusion coefficient D values of four rejuvenators in aged bitumen are derived using MATLAB with Eq.2 [54,55]. The measured and predicted D values are plotted together in Fig. 18 to validate the MD simulation outputs. It can be found that the measured D values depend on the characterization index type. For each rejuvenator, the difference in measured D values based on the rheological parameters of G^* , $G^*/\sin\delta$, $G^*\sin\delta$, $N_{f2.5}$, and $N_{f5.0}$ is slight, but the D values based on G-R and δ are smaller than others. Thus, the G-R and δ parameters are not appropriate for measuring the concentration distribution of rejuvenators in aged bitumen after a diffusion test. However, the magnitude of all measured D values of four rejuvenators is in the region of 10^{-11} - 10^{-10} m^2/s , which agrees with previous studies [23,25,28,53]. Therefore, according to the similar D values, one rheological index (such as G^* or N_f) is sufficient to determine the concentration distribution of rejuvenators in aged bitumen after a diffusion process.

From Fig. 18, the predicted D values of all rejuvenators from MD simulations are higher than the experimental results. In detail, the estimated D values of bio-oil, engine-oil, naphthenic-oil, and aromatic-oil rejuvenator in aged bitumen are almost 3.4, 2.9, 4.3, and 5.9 times larger than the corresponding experimental results.

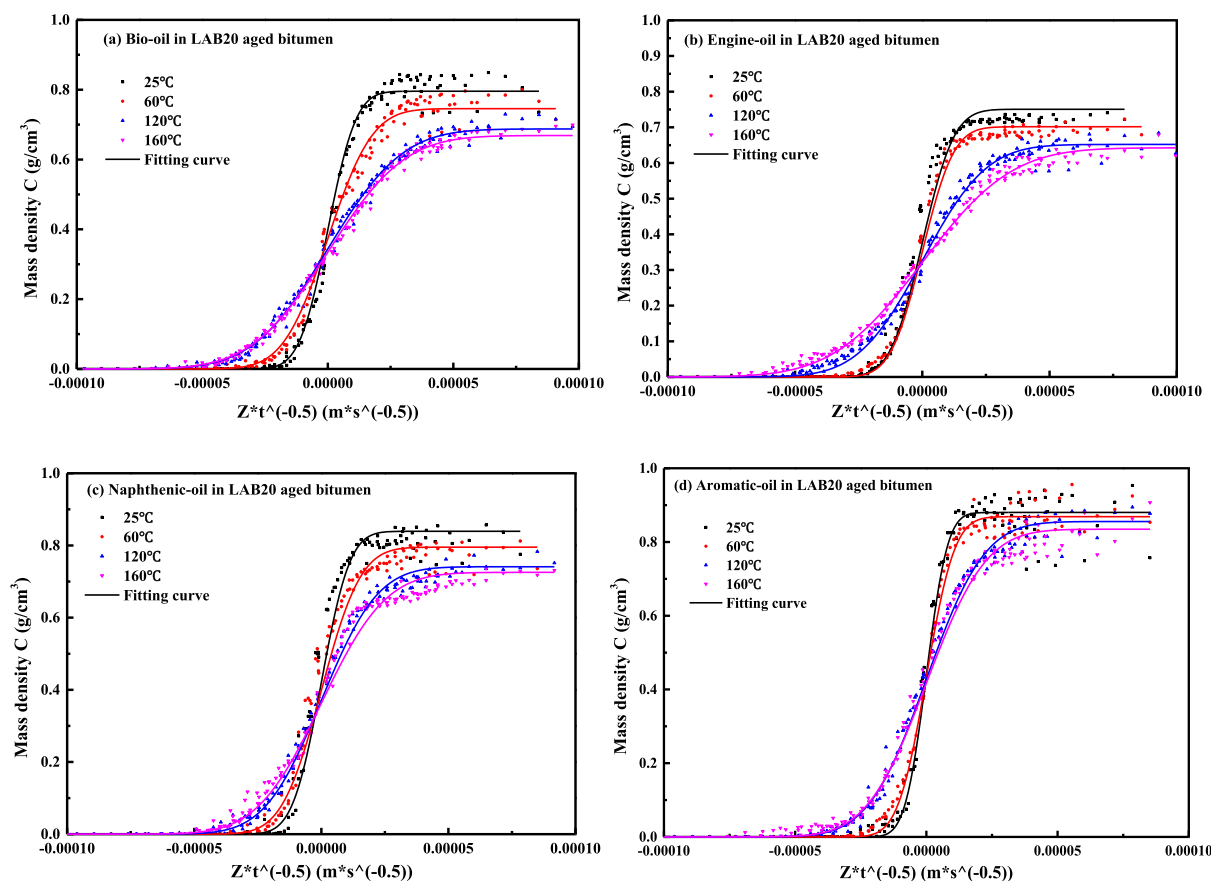


Fig. 21. Density profiles for rejuvenator molecules scaled with $zt^{0.5}$ in LAB20-aged bitumen.

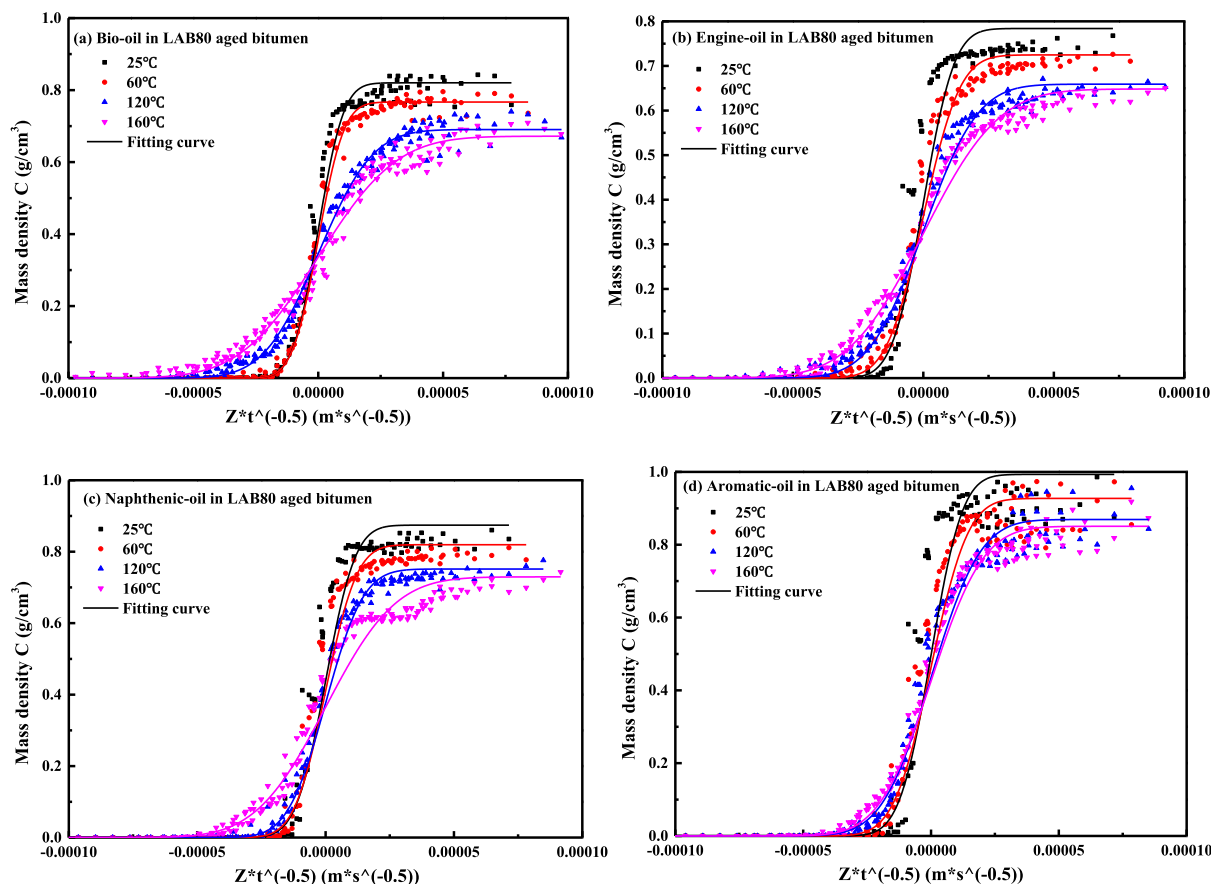


Fig. 22. Density profiles for rejuvenator molecules scaled with $zt^{0.5}$ in LAB80-aged bitumen.

The homogenization of diffusion layers at different positions would lead to experimental error. Meanwhile, the DSR test and concentration determination based on standard curves would also cause deviations to some extent. The predicted D values are directly derived from a density distribution profile of rejuvenator molecules in an aged bitumen model, which may be more accurate by preventing a concentration conversion procedure. On the other hand, there are still differences between MD simulation molecular models of aged bitumen and rejuvenators with their realistic chemical components and molecular structures.

All D values of four rejuvenators in aged bitumen from MD simulations and experimental tests are plotted in Fig. 19. The measured and predicted D values show the same trend for four rejuvenators as $BO > EO > NO > AO$. Moreover, it can be seen that the difference in D values between measured and predicted D values is dependent on the rejuvenator type. However, there is no apparent relationship between the measured and predicted D values for all rejuvenators. The measured D values based on G-R and δ parameters are far from the predicted D values. These four rejuvenators show diverse molecular structures, molecular weight and polarity, and intermolecular interaction with aged bitumen molecules. Therefore, the difference between the measured and predicted D values is inconsistent for all rejuvenators. It is worth noting that these rejuvenators in this study come from different categories, resulting in different degrees of difference between predicted and measured D values. Given this, it is recommended to compare the diffusion coefficient D values of various rejuvenators belonging to the same category (such as bio-oils, engine-oils,

naphthenic-oils, or aromatic-oils) and establish a potential relationship between the predicted and measured D values of different rejuvenator groups. Afterwards, a more efficient rejuvenator with a high diffusion capacity could be optimized from a molecular-scale perspective without any tedious experiment and trial process.

7. Influence of temperature and aging degree on diffusion behaviors of rejuvenators

According to the similarity in diffusion coefficient values, the MD simulation outputs are reliable and can accurately predict the diffusion behaviors of various rejuvenators in aged binders. The rejuvenator type, aging degree of bitumen, and temperature are considered in this MD simulation to study the diffusion characteristics of rejuvenator molecules in the aged bitumen model.

7.1. Molecular configurations of different diffusion models

Fig. 20 illustrates the molecular configurations of diffusion models with different rejuvenator types (BO, EO, NO, and AO) and aging degrees (LAB20, LAB40, and LAB80) at 60°C and 160°C. For all diffusion models, the rejuvenator molecules diffuse deeper in the aged bitumen at high temperatures, indicating that the increment of diffusion temperature promotes the blending between the rejuvenators and aged bitumen. Moreover, the diffusion trends of all the rejuvenators are limited to 60°C. Hence, the high mixing temperature and sufficient blending time are necessary to obtain a homogenous rejuvenated bitumen. The aging

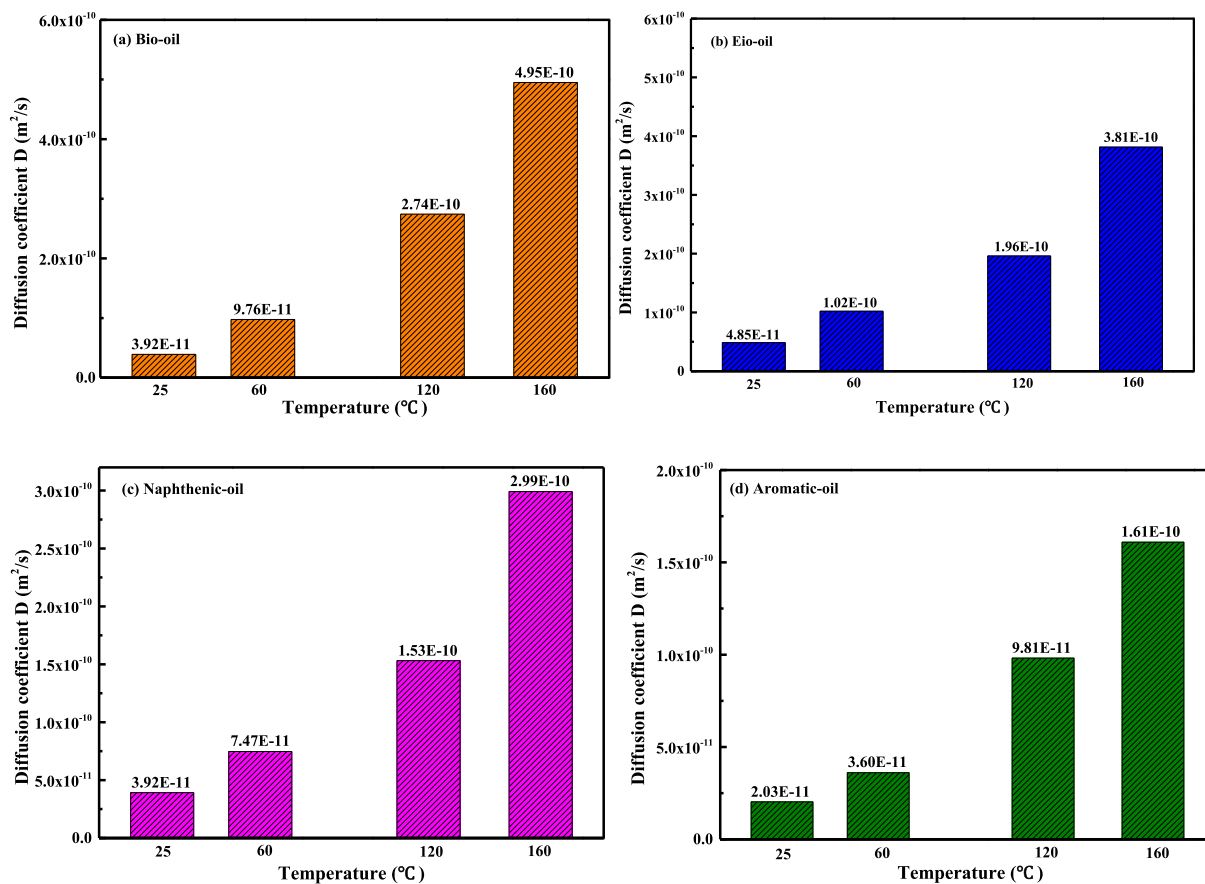


Fig. 23. Diffusion coefficient of rejuvenators in LAB20-aged bitumen versus temperatures.

degree of the aged bitumen significantly influences the diffusive capacity of rejuvenators in aged bitumen. Fewer rejuvenator molecules are observed in the aged bitumen layer when the aged bitumen changes from LAB20 to LAB40 and LAB80. It implies that as the aging degree increases, the penetration of rejuvenator molecules into the aged bitumen matrix is more challenging. This finding agrees well with the previous experimental results [21,49]. Meanwhile, the effect of the aging degree on the diffusive behaviors of rejuvenators is more apparent at high temperatures, but the temperature influence is more significant than the aging degree variation.

The underlying mechanisms at the molecular scale for the synergistic effects of temperature and aging degrees are complicated. As the aging degree increases, both the molecular weight and the polarity of bitumen molecules enlarge, which significantly enhances the intermolecular interaction and decreases the free volume of the aged bitumen model. Thus, it is more difficult for rejuvenator molecules to diffuse into the aged bitumen matrix. At the same time, the diffusion behavior between the rejuvenator and aged bitumen molecules is bidirectional, and the increased aging level leads to reduced molecular mobility of aged bitumen molecules. However, the coupled effects of temperature and aging degree on the diffusive capacity of rejuvenators in aged bitumen are dependent on the rejuvenator type. It is strongly related to the molecular structures of rejuvenators and the corresponding intermolecular interaction with the aged bitumen molecules.

On the one hand, the temperature effects on the molecular mobility of these rejuvenator molecules are distinctly different because of the difference in molecular structures. On the other

hand, the intermolecular force variations between the rejuvenators and aged bitumen molecules with different aging degrees are not the same. As the increase of aging level, the enlarged polarity of aged bitumen molecules would result in a more vital interaction with the bio-oil and aromatic-oil molecules with polar functional groups, but it shows a slight influence on the engine-oil and naphthenic-oil rejuvenators with less polarity. Nevertheless, it is not clear the fundamental role of intermolecular force between the rejuvenator and aged bitumen molecules in the diffusion behavior of the rejuvenator in a whole system. The solid intermolecular force would benefit from absorbing the rejuvenator molecules from the main rejuvenator phase and enlarging the blending level between the rejuvenator and aged bitumen. However, the high intermolecular interaction would result in the powerful adsorption of rejuvenator molecules on the surface of the aged bitumen and hinder more rejuvenator molecules from diffusing deeply into the aged bitumen layer. Here mainly focuses on the influence prediction of rejuvenator type, temperature, and aging degree on the whole diffusion rate of the rejuvenators in aged bitumen. More work should be conducted on the underlying mechanism at an atomic level in the future.

7.2. Density profiles for rejuvenator molecules in different aged binders

Figs. 21 and 22 illustrate the mass density distributions of different rejuvenators in LAB20-aged and LAB80-aged bitumen, respectively. The increment in diffusion temperature results in a high diffusion level of the rejuvenator in the aged bitumen model. When the temperature and aging degree keep constant, various

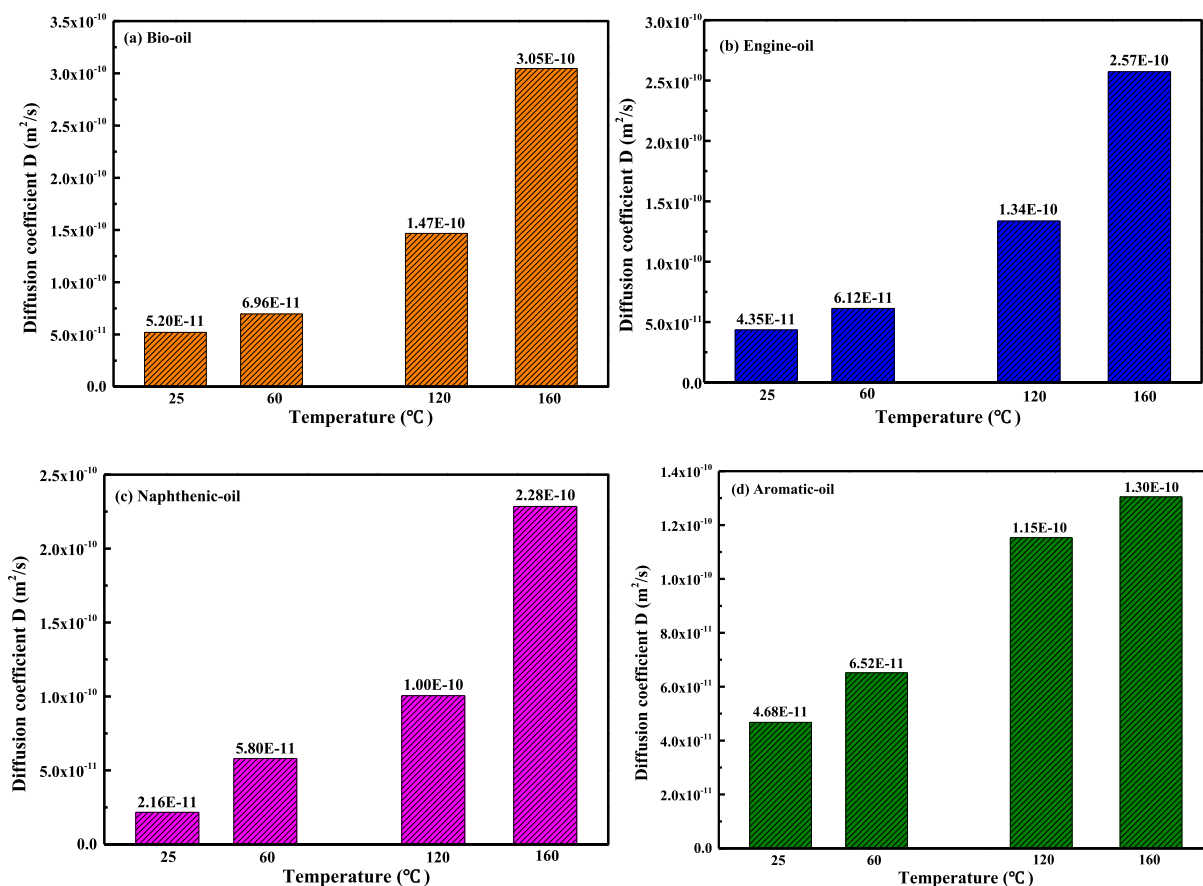


Fig. 24. Diffusion coefficient of rejuvenators in LAB80-aged bitumen versus temperatures.

rejuvenators exhibit different diffusion trends. The mass density of bio-oil molecules in the aged bitumen is the maximum, followed by the engine-oil and naphthenic-oil, while the minimum amount of aromatic-oil rejuvenator diffuses in the aged bitumen. Generally, the aged bitumen from nonidentical RAP resources shows different aging degrees and chemo-mechanical characteristics. Thus, comparing the relative concentrations of four rejuvenators in disparate RAP materials with various aged bitumen is interesting. Compared to LAB20-aged bitumen, the mass density of rejuvenator molecules in LAB80-aged bitumen is lower.

On the contrary, the rejuvenator concentration in the pure rejuvenator layer of these diffusion models containing LAB80-aged bitumen is much larger than that in LAB20-aged bitumen models. Therefore, it implies that the diffusion capacity of rejuvenators in the aged bitumen shows a reduction trend as the aging degree of aged bitumen increases. However, the mass density values of all the rejuvenators in LAB80-aged bitumen at 160°C are higher than that in LAB20-aged bitumen at 25 and 60°C. Therefore, it is concluded that the effect of temperature on the diffusion capacity of the rejuvenator in the aged bitumen is more significant than the aging degree. A high blending temperature is necessary to ensure sufficient rejuvenator diffusion in severely-aged bitumen within a limited mixing duration.

7.3. Diffusion coefficient of rejuvenator molecules in different aged binders

To further quantitatively assess the coupling effects of rejuvenator type, temperature, and aging degree on the interfacial diffusive behaviors of rejuvenator-aged bitumen systems, the

values of diffusion coefficient D of four rejuvenators in LAB20-aged and LAB80-aged bitumen at variable temperatures of 25, 60, 120, and 160°C are displayed in Figs. 23 and 24. Overall, the D values of all diffusion systems show an increasing trend with the temperature increasing. Moreover, the magnitude of D values for four rejuvenators is the same as $BO > EO > NO > AO$ at high temperatures of 120 and 160°C, regardless of the aging level of bitumen. However, this order is variable at low temperatures, which is also affected by the aging degree of bitumen. At both 25 and 60°C, for LAB20 and LAB40-aged bitumen, the engine-oil shows a higher D value than the bio-oil, followed by naphthenic-oil and aromatic-oil. The molecular mobility of both bio-oil and engine-oil is similar and limited at low temperatures [39,45]. However, the intermolecular forces between bio-oil and aged bitumen molecules are more substantial than the engine-oil, which would result in the interface adsorption of bio-oil, reduce the free volume in the aged bitumen surface, and thus prevent the deep diffusion of rejuvenator molecules into the aged bitumen matrix.

In addition, it is worth noting that the magnitude in D values for four rejuvenators in LAB80-aged bitumen differs from that in LAB20 and LAB40-aged binders at low temperatures of 25 and 60°C. The bio-oil and aromatic-oil molecules exhibit higher D values than the engine-oil and naphthenic-oil in severely-aged bitumen. In contrast, the aromatic-oil rejuvenator shows the smallest D values in slight-and-middle aged bitumen within the whole temperature range. It indicates that the aging degree of aged bitumen plays an essential role in affecting the diffusion behaviors of rejuvenators, especially for the aromatic-oil molecules with high polarity. The polarity in aged bitumen remarkably increases with the

increment in aging level, which enlarges the intermolecular interaction between the polar rejuvenators (aromatic-oil and bio-oil) and aged bitumen molecules. Afterward, the enhancement in the internal attraction force is beneficial to accelerate the diffusion behaviors of rejuvenator molecules from the rejuvenator phase to an aged bitumen matrix.

Fig. 25 demonstrates the significant influence of aging level on the D parameters of rejuvenators at various temperatures. As the aging degree of aged bitumen deepens, the D values of bio-oil, engine-oil, and naphthenic-oil molecules decrease, while the aromatic-oil exhibits an opposite behavior. For non-polar (engine-oil) and low-polar rejuvenators (naphthenic-oil), the increased aging level has little effect on their intermolecular force with aged bitumen molecules, but the reduction of free volume in aged bitumen presents a significantly negative influence on their diffusion behaviors. On the other hand, the D values of aromatic-oil molecules in aged bitumen rise gradually with the increment in aging level, indicating that the aromatic-oil rejuvenator diffuses faster in aged bitumen with a higher aging degree. Although bitumen aging reduces its free volume fraction, the enlarged polarity of bitumen molecules enhances the intermolecular interaction between the polar rejuvenator and aged bitumen molecules. That's why the aging level positively affects the diffusive capacity of the aromatic-oil rejuvenator. It should be mentioned that the adverse influence of aging level on the free volume fraction in the aromatic-oil diffusion model still exists, but the effect of enlarged intermolecular force on the diffusion rate is more significant than the reduced free volume factor. However, the D value of the

aromatic-oil rejuvenator at 160°C decreases with the aging level changes from LAB40 to LAB80. It means that the positive role of aging level on the diffusive capacity of aromatic-oil molecules due to the enhanced intermolecular force mainly occurs at low temperatures, and its adverse impacts on free volume fraction and diffusion coefficient value become more apparent as the temperature rises.

For bio-oil molecules, the aging level mainly adversely affects their diffusion behavior because of the reduction of free volume reduction. However, the D value at 25°C increases as the aging level changes from LAB40 to LAB80, indicating that the high aging degree improves the diffusive rate of bio-oil molecules in aged bitumen at low temperatures. Furthermore, there is a polar ester (O-C=O) functional group in the molecular structure of bio-oil, and the enlarged intermolecular force between the bio-oil and aged bitumen molecules at 25°C contributes more to improving its diffusion behavior than the negative effect of reduced free volume fraction. Lastly, it can be found that the aging level on the D parameters of rejuvenators in aged bitumen is also affected by the temperature and rejuvenator type. According to the downward or upward trend, the effects of the aging level on the D values of all rejuvenators are more significant at high temperatures. In addition, the influence level of the aging degree on D values of aromatic-oil molecules at low temperatures (25 and 60°C) is the maximum. At 120 and 160°C, the aging level shows a similar and most robust effect on D values of bio-oil and engine-oil, followed by the naphthenic-oil case, while this influence on aromatic-oil diffusion is the smallest.

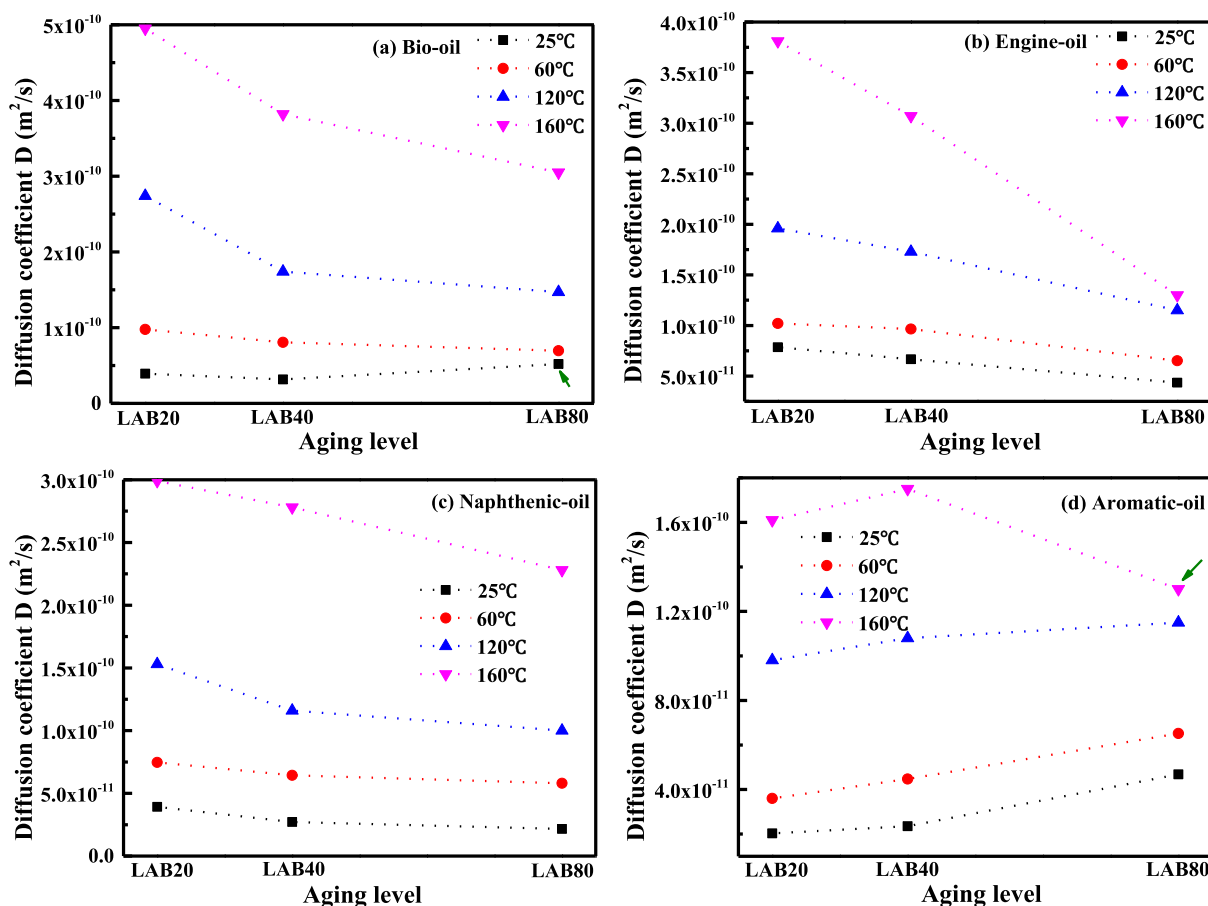


Fig. 25. Influence of aging level on the D values of four rejuvenators at different temperatures.

8. Conclusions and recommendations

8.1. Main conclusions

This study aims to observe the diffusion behaviors of four commonly-used rejuvenators in aged bitumen at an atomic level and predict their diffusive parameters at various temperatures using the MD simulation method. Moreover, the experimental diffusion method and rheological characterizations are conducted to validate the simulation outputs. Further, the synergetic effects of rejuvenator type, aging level of bitumen, and temperature on the diffusive capacity of the rejuvenator-aged bitumen interfacial model are explored and discussed. Some main findings are listed as follows:

(1) At an atomic scale, the mutual but partial interfacial diffusion behaviors between the rejuvenators and the aged bitumen molecules are observed. Meanwhile, high temperature and long diffusion time promote the diffusion level of all rejuvenators in the aged bitumen.

(2) Fick's Second Law well fits the concentration distribution of rejuvenator molecules in the aged bitumen matrix during various diffusion processes. Moreover, the diffusion coefficient D of four rejuvenators varies from 10^{-11} to 10^{-10} m²/s, which strongly depends on the rejuvenator type, temperature, and bitumen aging levels.

(3) In most cases, the order for the diffusive capacity of four rejuvenators is BO > EO > NO > AO. However, the engine-oil displays a higher D value than the bio-oil at low temperatures (25 and 60 °C), which may be related to the hindering influence of strong surface adsorption between the polar bio-oil and aged bitumen molecules at low temperatures. In addition, the diffusion behavior of bio-oil in the aged bitumen presents a higher temperature sensitivity than the other three rejuvenators.

(4) The experimental results in both the magnitude and order of D parameters agree well with the MD simulation outputs, but the predicted D values at 160°C of all rejuvenators are about 3–6 times larger than the measured values. Moreover, one rheological index (G^* or N_f , but no $G-R$ and δ parameters) is sufficient to determine the concentration distribution of the rejuvenator in the aged bitumen after a diffusion process.

(5) The increased aging degree exhibits a negative effect on the diffusion capacity of bio-oil, engine-oil, and naphthenic-oil rejuvenators in the aged bitumen, but the D value of an aromatic-oil molecule increases as the aging level deepens. The underlying mechanism may be composed of free volume fraction in the aged bitumen matrix and the intermolecular force between rejuvenator and aged bitumen molecules, which differs remarkably for various rejuvenators.

(6) The influence of the aging level on the temperature sensitivity of aromatic-oil diffusion behavior is the highest, followed by bio-oil, which is insignificant to the engine-oil and naphthenic-oil rejuvenators.

8.2. Recommendations for future research

This study verifies the possibility of MD simulation in predicting the diffusion capacity of different rejuvenators in the aged bitumen, considering the influence of rejuvenator types, temperatures, and aging degrees of bitumen. Furthermore, it would help us fundamentally understand the diffusion phenomenon of various rejuvenator-aged bitumen interface models at an atomic level. On the basis of the study's results, some recommendations are mentioned herein for future research.

- The molecular models of rejuvenators and aged bitumen should be further optimized according to their chemical characteristics to enhance the accuracy of MD simulation outputs.

- The diffusive parameters of rejuvenators can be measured from a low film thickness of the aged bitumen extracted from RAP collected from the field. In addition, the diffusion behaviors of rejuvenators in an aged-virgin bitumen double layer should be further investigated.
- The experimental validation work on the influence of temperature and bitumen aging level on the diffusion coefficient of rejuvenators can be performed.
- The potential connections between predicted and measured diffusive parameters of different rejuvenator-aged bitumen systems should be established for molecular-scale optimization of rejuvenators with a sufficient diffusion capacity.

CRediT authorship contribution statement

Shisong Ren: Methodology, Investigation, Formal analysis, Writing – original draft, Writing – review & editing. **Xueyan Liu:** Supervision, Writing – review & editing. **Yangming Gao:** Methodology, Supervision. **Ruxin Jing:** Methodology, Supervision. **Peng Lin:** Resources, Methodology, Supervision. **Sandra Erkens:** Methodology, Supervision. **Haopeng Wang:** Methodology, Supervision.

Data availability

Data will be made available on request.

Declaration of Competing Interest

The authors declare that they have no known competing financial interests or personal relationships that could have appeared to influence the work reported in this paper.

Acknowledgments

The first author would thank the China Scholarship Council for the funding support (CSC. No. 201906450025). Meanwhile, the corresponding author would thank the European Union's Horizon 2020 Research and Innovation Programme under the Marie Skłodowska-Curie grant agreement (No.101030767).

Appendix A. Supplementary data

Supplementary data to this article can be found online at <https://doi.org/10.1016/j.matdes.2023.111619>.

References

- [1] C.H. Domke, R.R. Davison, C.J. Glover, Effect of oxygen pressure on asphalt oxidation kinetics, *Ind. Eng. Chem. Res.* 39 (3) (2000) 592–598.
- [2] L. Ma, A. Vareri, R. Jing, S. Erkens, Comprehensive review on the transport and reaction of oxygen and moisture towards coupled oxidative ageing and moisture damage of bitumen, *Constr. Build. Mater.* 283 (2021) 122632.
- [3] J. Wu, Q. Liu, S. Yang, M. Oeser, C. Ago, Study on migration and diffusion during the mixing process of asphalt mixtures with RAP, *Road Materials and Pavement Design.* 22 (7) (2021) 1578–1593.
- [4] S. Ren, X. Liu, P. Lin, R. Jing, S. Erkens, Toward the long-term aging influence and novel reaction kinetics models of bitumen, *Int. J. Pavement Eng.* (2022), <https://doi.org/10.1080/10298436.2021.2024188>.
- [5] H.A. Ali, L. Mohammad, M. Mohammadafzali, F. Haddadi, M. Akentuna, G. Sholar, H. Moseley, W. Rilko, C. Allen, Investigating the effect of degree of blending on performance of high RAP content mixtures, *J. Mater. Civ. Eng.* 33 (4) (2021) 04021048.
- [6] S. Zhao, B. Huang, X. Shu, Investigation on binder homogeneity of RAP/RAS mixtures through staged extraction, *Constr. Build. Mater.* 82 (2015) 184–191.
- [7] Q. Liu, J. Wu, M. Oeser, Micro- and meso-scale homogeneity of asphalt mixtures with RAP in thermal-non-equilibrium condition, *Constr. Build. Mater.* 304 (2021) 124609.
- [8] S. Ren, X. Liu, H. Wang, W. Fan, S. Erkens, Evaluation of rheological behaviors and anti-aging properties of recycled asphalt using low-viscosity asphalt and polymers, *J. Clean. Prod.* 253 (2020) 120048.

- [9] M. Mohammadafzali, H. Ali, G.A. Sholar, W.A. Rilko, M. Baqersad, Effects of rejuvenation and aging on binder homogeneity of recycled asphalt mixtures, *Journal of Transportation Engineering, Part B: Pavements* 145 (1) (2019) 04018066.
- [10] Y. Ma, W. Hu, P.A. Polaczyk, B. Han, R. Xiao, M. Zhang, B. Huang, Rheological and aging characteristics of the recycled asphalt binders with different rejuvenator incorporation methods, *J. Clean. Prod.* 262 (2020) 121249.
- [11] Y. Fang, Z. Zhang, H. Zhang, W. Li, Analysis of wetting behavior and its influencing factors of rejuvenator/old asphalt interface based on surface wetting theory, *Constr. Build. Mater.* 314 (2022) 125674.
- [12] M. Zaumanis, L. Boesiger, B. Kunz, M.C. Cavalli, L. Poulikakos, Determining optimum rejuvenator addition location in asphalt production plant, *Constr. Build. Mater.* 198 (2019) 368–378.
- [13] M. Zaumanis, M.C. Cavalli, L. Poulikakos, Effect of rejuvenator addition location in plant on mechanical and chemical properties of RAP binder, *Int. J. Pavement Eng.* 21 (4) (2020) 507–515.
- [14] F.Y. Rad, N.R. Sefidmazgi, H. Bahia, Application of diffusion mechanism: degree of blending between fresh and recycled asphalt pavement binder in dynamic shear rheometer, *Transportation Research Record: Journal of the Transportation Research Board.* 2444 (2014) 71–77.
- [15] Y. Xiao, B. Yan, X. Zhang, X. Chang, M. Li, Study the diffusion characteristics of rejuvenator oil in aged asphalt binder by image thresholding and GC-MS tracer analysis, *Constr. Build. Mater.* 249 (2020) 118782.
- [16] M. Mohajeri, A.A.A. Molenaar, M.F.C. Van de Ven, Experimental study into the fundamental understanding of blending between reclaimed asphalt binder and virgin bitumen using nanoindentation and nano-computed tomography, *Road Materials and Pavement Design.* 15 (2) (2014) 372–384.
- [17] S.N. Nahar, M. Mohajeri, A.J.M. Schmets, A. Scarpas, M.F.C. van de Ven, G. Schitter, First observation of blending-zone morphology at interface of reclaimed asphalt binder and virgin bitumen, *Transportation Research Record: Journal of the Transportation Research Board.* 2370 (2013) 1–9.
- [18] G. Zou, J. Zhang, Y. Li, Z. Lin, Quantitative characterize binder blending and diffusion in recycled asphalt mixture: An environmental-friendly solution using wooden cube and 3D fluorescence image technology, *J. Clean. Prod.* 193 (2021) 126204.
- [19] S. Vassaux, V. Gaudefroy, L. Boulange, L. Jean Soro, A. Pevere, A. Michelet, V. Barragan-Montero, V. Mouillet, Study of remobilization phenomena at reclaimed asphalt binder/virgin binder interphases for recycled asphalt mixtures using novel microscopic methodologies, *Constr. Build. Mater.* 165 (2018) 846–858.
- [20] J. Xu, P. Hao, D. Zhang, G. Yuan, Investigation of reclaimed asphalt pavement blending efficiency based on micro-mechanical properties of layered asphalt binders, *Constr. Build. Mater.* 163 (2018) 390–401.
- [21] Y. He, Z. Alavi, J. Harvey, D. Jones, Evaluating diffusion and aging mechanisms in blending of new and age-hardened binders during mixing and paving, *Transportation Research Record: Journal of the Transportation Research Board.* 2574 (2016) 64–73.
- [22] R. Karlsson, U. Isacson, Application of FTIR-ATR to characterization of bitumen rejuvenator diffusion, *J. Mater. Civ. Eng.* 15 (2) (2003) 157–165.
- [23] G. Cuciniello, N. Mallegni, M. Cappello, S. Filippi, P. Leandri, G. Polacco, M. Losa, Classification and selection of exhausted oils for rejuvenating bituminous blends, *Constr. Build. Mater.* 278 (2021) 122387.
- [24] Y. Fang, Z. Zhang, J. Shi, X. Yang, X. Li, Insights into permeability of rejuvenator in old asphalt based on permeation theory: Permeation behaviors and micro characteristics, *Constr. Build. Mater.* 325 (2022) 126765.
- [25] T. Ma, X. Huang, Y. Zhao, Y. Zhang, Evaluation of the diffusion and distribution of the rejuvenator for hot asphalt recycling, *Constr. Build. Mater.* 98 (2015) 530–536.
- [26] M. Xu, J. Yi, D. Feng, Y. Huang, Diffusion characteristics of asphalt rejuvenators based on molecular dynamics simulation, *Int. J. Pavement Eng.* 20 (5) (2019) 615–627.
- [27] G. Xu, H. Wang, Diffusion and interaction mechanism of rejuvenating agent with virgin and recycled asphalt binder: a molecular dynamics study, *Mol. Simul.* 44 (17) (2018) 1433–1443.
- [28] W. Sun, H. Wang, Molecular dynamics simulation of diffusion coefficients between different types of rejuvenator and aged asphalt binder, *Int. J. Pavement Eng.* 21 (8) (2020) 966–976.
- [29] H. Ding, H. Wang, X. Qu, A. Varveri, J. Gao, Z. You, Towards an understanding of diffusion mechanism of bio-rejuvenators in aged asphalt binder through molecular dynamics simulation, *J. Clean. Prod.* 126977 (2021).
- [30] H.F. Haghshenas, R. Rea, G. Reinke, D.F. Haghshenas, Chemical characterization of recycling agents, *J. Mater. Civ. Eng.* 32 (5) (2020) 06020005.
- [31] H.F. Haghshenas, R. Rea, G. Reinke, M. Zaumanis, E. Fini, Relationship between colloidal index and chemo-rheological properties of asphalt binders modified by various recycling agents, *Constr. Build. Mater.* 318 (2022) 126161.
- [32] ASTM D5-06. Standard Test Method for Penetration of Bituminous Materials.
- [33] ASTM D36-06. Standard Test Method for Softening Point of Bitumen (Ring and Ball Apparatus).
- [34] AASHTO T316-13. Standard Method of Test for Viscosity Determination of Asphalt Binder Using Rotational Viscometer.
- [35] EN 15326. British Standard for Bitumen and Bituminous Binders-measurement of Density and Specific Gravity-capillary-stoppered Pycnometer Method.
- [36] ASTM D4124-01. Standard Test Methods for Separation of Asphalt into Four Fractions.
- [37] ASTM D7343. Standard Practice for Optimization, Sample Handling, Calibration, and Validation of X-ray Fluorescence Spectrometry Methods for Elemental Analysis of Petroleum Products and Lubricants.
- [38] AASHTO M 320. Standard Specification for Performance-graded Asphalt Binder.
- [39] S. Ren, X. Liu, S. Erkens, P. Lin, Y. Gao, Multi-component analysis, molecular model construction, and thermodynamics performance prediction on various rejuvenators of aged bitumen, *J. Mol. Liq.* 119463 (2022).
- [40] ASTM D1754. Standard Test Method for Effect of Heat and Air on Asphaltic Materials. (Thin-Film Oven test).
- [41] AASHTO R28. Standard Method of Test for Accelerated Aging of Asphalt Binder Using a Pressurized Aging Vessel (PAV).
- [42] P. Cong, H. Hao, Y. Zhang, W. Luo, D. Yao, Investigation of diffusion of rejuvenator in aged asphalt, *Int. J. Pavement Res. Technol.* 9 (4) (2016) 280–288.
- [43] AASHTO TP 101. Standard Method of Test for Estimating Fatigue Resistance of Asphalt Binders Using the Linear Amplitude Sweep.
- [44] S. Ren, X. Liu, P. Lin, S. Erkens, Y. Xiao, Chemo-physical characterization and molecular dynamics simulation of long-term aging behaviors of bitumen, *Constr. Build. Mater.* 302 (2021) 124437.
- [45] S. Ren, X. Liu, P. Lin, S. Erkens, Y. Gao, Chemical characterizations and molecular dynamics simulations on different rejuvenators for aged bitumen recycling, *Fuel* 324 (2022) 124550.
- [46] Y. Gao, Y. Zhang, C. Zhang, X. Liu, R. Jing, Quantifying oxygen diffusion in bitumen films using molecular dynamics simulations. 331 (2022) 127325.
- [47] M. Zadsheer, D.J. Oldham, S. Hosseini-zhad, E.H. Fini, Investigating bio-rejuvenation mechanisms in asphalt binder via laboratory experiments and molecular dynamics simulation, *Constr. Build. Mater.* 190 (2018) 392–402.
- [48] Y. Ding, B. Huang, X. Shu, Y. Zhang, M.E. Woods, Use of molecular dynamics to investigate diffusion between virgin and aged asphalt binders, *Fuel* 174 (2016) 267–273.
- [49] R. Karlsson, U. Isacson, Bitumen rejuvenator diffusion as influenced by ageing, *Road Materials and Pavement Design.* 3 (2) (2002) 167–182.
- [50] W.S. Mogawer, A. Booshehrian, S. Vahidi, A.J. Austerman, Evaluating the effect of rejuvenators on the degree of blending and performance of high RAP, RAS, and RAP/RAS mixture, *Road Materials and Pavement Design.* 14 (2) (2013) 193–213.
- [51] B.F. Bowers, B. Huang, X. Shu, B.C. Miller, Investigation of reclaimed asphalt pavement blending efficiency through GPC and FTIR, *Constr. Build. Mater.* 50 (2014) 517–523.
- [52] M. Li, L. Liu, C. Xing, L. Liu, H. Wang, Influence of rejuvenator preheating temperature and recycled mixture's curing time on performance of hot recycled mixtures, *Constr. Build. Mater.* 295 (2021) 123616.
- [53] M. Xu, Y. Zhang, Study of rejuvenators dynamic diffusion behavior into aged asphalt and its effects, *Constr. Build. Mater.* 261 (2020) 120673.
- [54] Y. Gao, Y. Zhang, Y. Yang, J. Zhang, F. Gu, Molecular dynamics investigation of interfacial adhesion between oxidized bitumen and mineral surfaces, *Appl. Surf. Sci.* 479 (2019) 449–462.
- [55] Y. Gao, Y. Zhang, F. Gu, T. Xu, H. Wang, Impact of minerals and water on bitumen-mineral adhesion and debonding behaviours using molecular dynamics simulations, *Constr. Build. Mater.* 171 (2018) 214–222.